Coordinated Cluster and ground-based instrument observations of transient changes in the magnetopause boundary layer during an interval of predominantly northward IMF: relation to reconnection pulses and FTE signatures

M. Lockwood [1,2], A. Fazakerley [3], H. Opgenoorth [4], J. Moen [5,6], A.P. van Eyken [7], M. Dunlop [14], J.-M. Bosqued [8], G. Lu [9], C.Cully[17], P. Eglitis [4], I.W. McCrea [1], M.A. Hapgood [1], M.N. Wild [1], R. Stamper [1], W. Denig [15], M. Taylor [3], J.A. Wild [10], G. Provan [10], O. Amm [11], K. Kauristie [11], T. Pulkkinen [11], A. Strømme [12], P. Prikryl [13], F. Pitout [4], A. Balogh [14], H. Rème [8], R. Behlke [4], T. Hansen [12], R. Greenwald [16], H. Frey[21], S.K. Morley [2], D. Alcayde [8], P.-L. Blelly [8], E. Donovan[17], M. Engebretson [18], M. Lester [10], J. Waterman [19], M.F. Marcucci [20]

[1] Solar Terrestrial Physics Division, Space Science and Technology Department, Rutherford Appleton Laboratory, Chilton, Didcot, Oxfordshire, UK
[2] Department of Physics and Astronomy, Southampton University, Southampton, UK
[3] Mullard Space Science Laboratory, Holmbury St. Mary, Surrey, UK
[4] IRF, Swedish Institute of Space Physics, Uppsala Division
[5] Department of Physics, University of Oslo, Blindern, Oslo, Norway.
[6] Also at Arctic Geophysics, University Courses on Svalbard, Longyearbyen, Norway.
[7] EISCAT Scientific Association, Longyearbyen, Svalbard, Norway
[8] CESR, Centre d'Etude Spatiale des Rayonnements, Toulouse, France
[9] High Altitude Observatory, National Center for Atmospheric Research, Boulder, Colorado, USA
[10] Department of Physics and Astonomy, Leicester University, Leicester, UK
[11] Finnish Meteorological Institute, Helsinki, Finland
[12] University of Tromsø, Tromsø, Norway
[13] Communications Research Centre, Ottawa, Ontario, Canada
[14] Blackett Laboratory, Imperial College, London, UK
[15] AFRL, Hanscom AFB, Cambridge, MA, USA
[16] Remote Sensing Group, Applied Physics Laboratory, John Hopkins University, Laurel, MD, USA
[17] University of Calgary, Calgary, Canada
[18] Department of Physics, Augsburg College, Minneapolis, MN, USA
[19] Danish Meteorological Institute, Kobenhavn, Denmark
[20] Istituto di Fisica dello Spazio Interplanetario – CNR, Rome, Italy
[21] Space Science Centre, Berkeley

Abstract. We study a series of transient entries into the low-latitude boundary layer (LLBL) of all four Cluster craft during an outbound pass through the mid-afternoon magnetopause ($[X_{GSM}, Y_{GSM}, Z_{GSM}] \approx [2, 7, 9]$ R_E). The events take place during an interval of northward IMF, as seen in data from the ACE satellite and lagged by a propagation delay of 75 min that is well defined by two separate studies: (1) of the magnetospheric variations prior to the northward turning (*Lockwood et al.,* 2001, this issue) and (2) of the field clock angle seen by Cluster after it had emerged into the magnetosheath (*Opgenoorth et al.,* 2001, this issue). With an additional lag of 16.5 min, the transient LLBL events correlate well with swings of the IMF clock angle (in GSM) to near 90°. Most of this additional lag is explained by ground-based observations, which reveal signatures of transient reconnection in the pre-noon sector that then take 10-15 min to propagate eastward to15 MLT, where they are observed by Cluster. The eastward phase speed of these signatures agrees very well with the motion deduced by cross-correlation of the signatures seen on the four Cluster craft. The evidence that these events are reconnection pulses includes: transient erosion of the noon 630 nm (cusp/cleft) aurora to lower latitudes; transient and travelling enhancements of the flow into the polar cap, imaged by the AMIE technique; and poleward-moving events moving into the polar cap, seen by the EISCAT Svalbard Radar (ESR). A pass of the DMSP-F15 satellite reveals that the open field lines near noon have been opened for some time: the more recently opened field lines were found nearer dusk where the flow transient and the poleward-moving event intersected the satellite pass. The events at Cluster have ion and electron characteristics predicted and observed by *Lockwood and Hapgood* (1998) for a Flux Transfer Events (FTE), with allowance for magnetospheric ion reflection off Alfvénic disturbances in the magnetopause reconnection layer. Like FTEs, the events are about $1R_E$ in their direction of motion and show a rise in the magnetic field strength but, unlike FTEs, in general they show no pressure excess in their core and hence no characteristic bipolar signature in the boundary-normal component. However, most of the events were

observed where the magnetic field was southward, i.e. on the edge of the interior magnetic cusp, or when the field was parallel to the magnetic equatorial plane. Only when the satellite begins to emerge into the exterior boundary (where the field was northward), do the events start to show a pressure excess in their core and the consequent bipolar signature. We identify the events as the first observations of flux transfer events at middle altitudes.

1. Introduction

The low-latitude boundary layer (LLBL) is characterised by the presence of both magnetosheath and magnetospheric plasma, inside the main magnetopause current sheet (*Hones et al.*, 1972; *Akasofu et al.*,1973; *Eastman et al.*, 1976; *Haerendel et al.*, 1978; *Eastman and Hones*, 1979; *Sonnerup*, 1980; *Sckopke et al.*, 1981; *Mitchell et al.*, 1987; *Hapgood and Bryant*, 1990; *Gosling et al.*, 1990a, b, c; *Song et al.,* 1990; *Skopke*, 1991; *Traver et al.*, 1991; *Fuselier et al.*, 1992; *Woch and Lundin*, 1993; *Woch et al.*, 1993; *Saunders*, 1993; *Hapgood and Lockwood*, 1993, 1995; *Phan et al.*, 1997; *Savin et al.*, 1997; *Fujimoto et al.*, 1998) . The origin of this layer is one of the major unanswered questions in magnetospheric physics and a key unknown in this regard is the topology of the LLBL field lines: it is interesting to note that roughly half of the papers cited above interpret the LLBL in terms of closed field lines, and the other half in terms of open field lines. There are three main classes of theory of LLBL formation (see review by *Sibeck et al.,* 1999). (1) magnetosheath plasma is injected by some process (such as wave-driven diffusion) onto closed field lines that are already populated with magnetospheric plasma (*Drakou*, 1994; *Lotko and Sonnerup*, 1995; *Treumann et al.*, 1991, 1995; *Winske et al.*, 1995). (2) The plasma mixture arises on newly-opened field lines along which magnetosheath plasma has flowed into the magnetosphere but magnetospheric plasma has yet to escape, either because of time-of-flight considerations (*Lockwood and Smith*, 1993; *Onsager*, 1994; *Lockwood*, 1997a; b; *Fuselier et al.*, 1999; *Onsager and*

Lockwood, 1999), or ion reflection at the reconnection layer Alfvén waves (*Cowley*, 1982; *Lockwood et al*., 1996) or because a magnetic bottle still exists on open field lines (*Daly and Fritz*, 1982; *Scholer et al*., 1982a; *Cowley and Lewis,* 1990, *Lyons et al.*, 1994). (3) The field lines of the LLBL had been open, allowing magnetosheath plasma to enter, but have subsequently been re-closed by re-reconnection (*Nishida*, 1989; *Song and Russell*, 1992; *Song et al.*, 1994; *Richard et al.*, 1994). In both (2) and (3) gradient and curvature drift across the open-closed boundary may sometimes help to replenish magnetospheric plasma that has been lost by flowing across the magnetopause along open field lines.

1-i Middle and low altitude signatures of the LLBL

As well as observations made at the magnetopause, data from middle- (*Woch et al.,* 1993, 1994) and low- (*Newell and Meng*, 1988; 1992) altitudes have been used to discuss the LLBL, the "cleft" precipitation often being thought of a the field-aligned projection of the LLBL (*Vasyluinas*, 1979; *Newell and Meng*, 1988; 1989; 1992; 1993; 1994a; Newell et al., 1991). However, this concept does not allow for two important considerations. Firstly, the low-altitude observations are of particles that are within the loss cone and the magnetopause observations are of particles that are mainly outside of the lost cone. Thus the low-altitude observations of the LLBL require that the loss cone is being filled and this need not be true of the magnetopause observations. Thus, for example, the mechanism proposed by *Song and Russell* (1992) will not yield a low-altitude LLBL (the filling of the loss cone with magnetosheath plasma ceasing when the field lines are re-closed), unless one also invokes strong pitch angle scattering of trapped particles on the re-closed field line into the loss cone. Secondly, such field-line mapping does not allow for the effects of velocity dispersion which is significant for ions in a convecting magnetosphere (*Rosenbauer et al.,* 1975; *Reiff et al.,* 1977). This dispersion does not allow the LLBL boundaries at high altitudes to be mapped to low altitudes whenever there is convective flow across that boundary (*Lockwood and Smith*, 1993). Because observations of dayside

convection show flow into the polar cap throughout much of the dayside (e.g. *Jorgensen et al.*, 1984), usually without a pronounced restriction or throat (*Heelis et al.,* 1976), this appears to be the case for a large fraction of the dayside. The open magnetosphere model predicts that the precipitation at low altitudes evolves in its classification from "LLBL/cleft" to "cusp" to "mantle" and then to "polar cap" as the field line evolves over the magnetopause away from the reconnection site and into the tail lobe (*Cowley et al.*, 1991; *Lockwood and Smith*, 1993, 1994; *Onsager et al.*, 1993; *Lockwood,* 1995). This evolution is seen in full along the flow streamlines in the steady state case and thus may sometimes be seen if the satellite follows the flow streamline quite closely (*Onsager et al.,* 1993; *Lockwood et al.,* 1994). Thus several authors have argued that much of the low-altitude LLBL precipitation must be on open field lines (*Lockwood and Smith*, 1993; *Lyons et al.*, 1994; *Moen et al*., 1996; *Fuselier et al.,* 1991; 1992; 1999). Others, whilst accepting that this is true where reconnection is taking place, now argue that there is also a closed LLBL at low altitudes nearer dawn and dusk (*Newell and Meng*, 1997). *Lockwood* (1997a) has shown how adopting an open topology for the LLBL solves a number of long-standing anomalies.

That the low-altitude signature of what is termed the LLBL is on open field lines is supported by the fact that it covers roughly the same longitudinal extent as the low-altitude mantle (*Newell and Meng*, 1992), which is known to be on open field lines (*Xu* et al., 1995). The longitudinal extent of the cusp is lower than that of both the LLBL and mantle (*Aparicio et al.,* 1991; *Newell and Meng*, 1992) and would be set by the longitudinal variation of sheath plasma concentration (*Lockwood,* 1997a). In addition, studies of the voltage across regions of low-altitude LLBL precipitation in both hemispheres (*Lu et al.*, 1994) show that on any one flank (dawn or dusk) the same voltage does not always appear in the two hemispheres: we interpret this as indicating that at least some of the flank low-altitude LLBL was on open and not closed field lines in these cases. Some observations also show LLBL-like precipitation on sunward-convecting field lines (*Nishida et al.,* 1993; *Nishida and*

Mukai, 1994). There is some debate as to whether these are truly LLBL field lines (*Newell and Meng* ,1994b) but, if so, the sunward convection can be explained in terms of the curvature force on open field lines but is inconsistent with mechanisms that transfer sheath plasma and momentum onto closed field lines.

1-ii The open LLBL at the magnetopause

Observations confirm the existence of an "open LLBL" (a term hereafter used for an LLBL inside which the field lines have an open topology) at the magnetopause. This type of LLBL is characterised by accelerated flows of magnetosheath-like ions. The evidence that they are injected and accelerated by flowing along newly-opened field lines includes: an observed dependence of the east-west flow direction on the IMF B_y component and hemisphere (*Gosling et al.,* 1990a); results of tangential stress balance tests (*Paschmann et al.*, 1979; 1986; *Sonnerup et al.*, 1981; 1986; *Johnstone et al.*, 1986); observations of D-shaped distribution functions of injected ions (*Smith and Rodgers*, 1991; *Fuselier et al.*, 1991; *Gosling et al.*, 1990b; c) as predicted by *Cowley* (1982); the observation of magnetosheath electron and ion edges inside the magnetic field rotational discontinuity (*Gosling et al.*, 1990c); depleted populations of trapped particles (*Scholer et al.*, 1982a; *Daly and Fritz*, 1982). The observations by *Fuselier et al.* (1991) show that the ion distributions on both sides of the magnetopause of both magnetospheric and magnetosheath origin are as predicted by the theory of plasma mixing along open field lines. In addition, *Smith and Rodgers* (1991) applied the stress-balance test to show that the low-velocity cut-off of the injected sheath population was close to the local de-Hoffman Teller frame velocity, as also predicted by the theory. Thus at least part of the magnetopause LLBL is formed by plasma mixing on field lines opened by magnetopause reconnection. Such processes could act for all IMF orientations, for example a reconnection site at high latitudes above the magnetic cusp, of the

kind studied by *Gosling et al.* (1991), has been seen to give rise to a dayside LLBL (*Paschmann et al.*, 1990).

At this point we should clarify some semantic points about nomenclature. Some authors would not term an open field line region "LLBL" at all, instead using the term "accelerated flows" or "reconnection layer" , as envisaged by *Levy et al*. (1964), *Heyn et al.,* (1988) and *Lin and Lee* (1993) and reserving the term LLBL for a layer on closed field lines. In addition, the open LLBL produced by lobe reconnection has also been referred to as an "overdraped lobe" (*Crooker*, 1992).

1-iii. The closed LLBL at the magnetopause

Many researchers have discussed an LLBL on closed field lines (see review by *Lotko and Sonnerup*, 1995). Because the LLBL was found to generally flow faster away from the subsolar point (*Haerendel et al.,* 1978), along with indications that it was also thicker there (*Mitchell et al.*, 1987; *Manuel and Samson*, 1993), *Eastman and Hones* (1979) suggested that the LLBL was formed by diffusion of magnetosheath plasma across the magnetopause. However, *Sonnerup* (1980) pointed out that the observed waves were not adequate to drive the required diffusion, a finding confirmed by later studies (*Owen and Slavin*, 1992*; LaBelle and Treumann*, 1988; *Winske et al*., 1995; *Treumann et al.*, 1995). Other mechanisms have been proposed for particle injection onto a closed LLBL but found to be either invalid or inadequate, for example, one proposed impulsive penetration mechanism has been demonstrated to be theoretically unsound (*Owen and Cowley*, 1991).

Nishida (1989) proposed a mechanism whereby reconnection may be responsible for plasma populations on a closed LLBL when the IMF points northward. He invoked highly patchy reconnection such that field lines opened at one reconnection site were re-closed a short time later time elsewhere. During the time

that the field line was open, magnetosheath plasma was free to flow in and magnetosphere plasma flowed out, giving the observed plasma mixture which is trapped when the field line is closed again. More recently, *Song and Russell* (1992) and *Song et al.* (1994) proposed a similar mechanism, but involving only two large-scale lobe reconnection sites, poleward of the magnetic cusps. Numerical simulations by *Richard et al.* (1994) indicate that magnetosheath plasma may indeed get onto closed field lines in this way during intervals of northward IMF.

1-iv "Subsolar" reconnection during northward IMF

Another possibility is that low-latitude reconnection may often be maintained during periods of northward IMF, as it is during southward IMF. The term "low –latitude" here means that the reconnection site is between the magnetic cusps such that it generates new open flux from closed flux. Studies of transpolar voltage as a function of IMF orientation show that the rate of production of such LLBL field lines must be low during northward IMF (*Reiff and Luhmann*, 1986; *Cowley*, 1984; *Freeman et al.*, 1993; *Boyle et al.,* 1997), nevertheless it may be sufficient to produce an open LLBL even during northward IMF, especially if the IMF clock angle θ_{IMF} is not too small (typically $> 45°$). Evidence for this comes from electron and ion distribution functions and flows in the LLBL (*Onsager and Fuselier*, 1994; *Fuselier et al.*, 1995; *Chandler et al.*, 1999). In addition, studies of the cusp aurora during weakly northward IMF show evidence for continued low-latitude reconnection, in addition to lobe reconnection (*Sandholt et al.*, 1997). Such reconnection during northward IMF was also deduced by Nishida et al (1998) from tail observations made by the GEOTAIL satellite. One possibility, suggested by *Anderson et al.* (1997), is that the magnetosheath field is distorted and amplified in the plasma depletion layer (which is less readily eroded during northward IMF) and this allows low-latitude reconnection to continue even when the upstream IMF points northward. Recent work shows that if the IMF vector has a northward

component but lies with about 45º of the magnetic equatorial plane ($45 < \theta_{IMF} < 90°$), the cusp/cleft aurora bifurcates into two bands (*Sandholt et al.*, 1996; 1998; 1999; *Lockwood and Moen*, 1999). The higher latitude part is consistent with the reconfiguration of "old" open flux by reconnection at the lobe magnetopause. There are two possible origins of the lower latitude band: it could be the signature of loss cone refilling of a closed northward-IMF LLBL or it could be on newly opened field lines that are produced by continued subsolar reconnection, despite the northward IMF component (probably at a different MLT to the lobe reconnection site). *McCrea et al.*, (2000) observed the equatorward erosion of the lower-latitude band using EISCAT radar data and this argues for the reconnection origin and an open LLBL.

Hall et al. (1991) find that the counterstreaming electrons, often used to define the LLBL (for example, *Takahashi et al.*, 1991) are present most all the time on most of the dayside magnetopause. *Lockwood and Hapgood* (1997, 1998) have used the ion observations and tangential stress balance tests to show that they are well explained as being the response of the electron gas to ion flight time effects, required to maintain quasi-neutrality on newly-opened field lines (*Burch*, 1985). The fact that these electron streams are seen during both southward and northward IMF therefore implies that reconnection is nearly always taking place somewhere on the magnetopause and is able to coat most of the boundary with newly-reconnected field lines and thus counterstreaming injected sheath electrons.

1-v. Distinguishing of open and closed models of the LLBL.

Making the distinction between closed and open field lines from observations of the LLBL is notoriously difficult, but has usually rested on the forms of the particle distribution functions. It has been argued that particle distributions often used to classify field lines as closed, can arise simply in the open magnetosphere model.

This does not necessarily mean all of the LLBL is on open field lines, but it does imply that more of it may be than has previously been thought. In an open LLBL, the particle populations vary with time elapsed since the field line was reconnected. This means that any reconnection rate changes will result in spatial structure ("cusp ion steps") in the open LLBL and cusp (*Lockwood and Hapgood*, 199; 1998). This concept has been used successfully to explain spatially structured magnetosheath ion precipitation at lower altitudes (*Lockwood and Smith*,1992, 1994; *Lockwood and Davis*,1996; *Lockwood et al*, 1998).

There is a good reason to be searching for a unified mechanism for a particle injection into the LLBL and a single magnetic topology within the LLBL. *Hapgood and Bryant* (1992) have shown that electron temperature varies in a consistent and repeatable manner with electron density throughout nearly all magnetopause crossings. Fluctuations in the time series of both quantities are produced by magnetopause motions, but these are effectively caused by the satellite moving back and forth along what is a continuous transition in the boundary rest frame. Such a transition, seen in the moments of the electron gas, could be present for almost any process that causes mixing of the magnetospheric and magnetosheath populations. What is significant, however, is that using these electron data to indicate the satellite's relative position in the LLBL (the "transition parameter"), reveals coherent structure in both the ion flows and magnetic field, which are independent of the electron measurements (*Hapgood and Bryant*, 1992; *Hapgood and Lockwood*, 1993). Recently, *Lockwood and Hapgood* (1997) have shown that the transition parameter (the degree of electron mixing) bears a simple relationship to time-elapsed since reconnection, showing that it works because there are open field lines coating the magnetospheric surface, i.e. an open LLBL. This being the case, the most significant point is that the transition parameter ordering is effective for nearly all passes in all parts of the LLBL, producing coherent variations through structures like flux transfer events and accelerated flow events, as well as seemingly closed LLBL field lines (*Hapgood*

and Lockwood, 1995). It is difficult to see how the smooth coherent structure could be achieved by a variety of mechanisms.

The identification of closed LLBL field lines has usually rested on two features, namely trapped magnetospheric particles and bi-directional streaming electrons.

1-vi. Trapped particles

Trapped particles, with a double loss cone pitch-angle distributions, arise on closed field lines connecting to both ionospheres. The particles are trapped between the mirror points in the two hemispheres. The problem with using such distributions to determine the status of a field line is that they can also exist on open field lines for a number of reasons.

Firstly, a magnetospheric population is not lost as soon as the field line is opened. This is not just because of time-of-flight effects: the theory of *Cowley* (1982), as verified by observations by *Smith and Rodgers* (1990), *Fuselier et al.* (1991) and *Fedorov et al.* (1999), predicts that of order one half of the population of magnetospheric ions incident on the magnetopause on an open field line is reflected back into the magnetosphere, in such a way as to conserve the pitch angle distribution. *Lockwood* (1997b) has shown how these reflected ions can combine with those that have yet to interact with the magnetopause to produce a population that appears as an undisturbed magnetospheric population. This would be seen on the same open field lines on which magnetosheath plasma is detected. The reflection also gives energised ions that are often seen in the LLBL and cusp (*Hill and Reiff*, 1977; *Alem and Delcourt*, 1995; *Moen et al.,* 1995; *Kremser et al*., 1995; *Lockwood*, 1997b).

Lockwood et al. (1996) proposed that ions can be reflected of bot the interior and exterior Alfvén waves (Rotational discontinuities) that stand in the inflows to the reconnecting magnetopause from, respectively, the magnetosphere and the

magnetosheath. Because the plasma concentration is low in the magnetosphere, the interior RD propagates at a high Alfvén speed and reflection of ions off it can give the considerable ion energisation sometimes found in the LLBL (Williams et al., 1987). Including this ion reflection, *Lockwood and Moen* (1995) and *Lockwood* (1997b) were able to get very good matches to the ion data from the LLBL presented by *Moen et al.* (1995) and *Kremser et al.*, (1995), respectively.

In addition, there may be a local maximum in the magnetic field strength near the point where the field line threads the boundary and/or the bow shock, and thus there can be a magnetic bottles on open field lines (*Cowley and Lewis*, 1990) which maintains quasi-trapped double loss cone distributions of both ions and electrons (*Scholer et al.*, 1982; *Daly and Fritz*, 1982). Another factor may be that energetic, large pitch angle ions and electrons can gradient-B and curvature-B drift onto open field lines. Such penetration of the open field line region by magnetospheric particles would be on the dawn side for electrons and on the dusk side for ions.

1-vii. Bi-directional streaming electrons

The LLBL also is often found to contain bi-directional field-aligned streams of electrons with energies of typically 20-500 eV (*Ogilvie et al.*, 1984; *Hall et al.*, 1991; *Traver et al.*, 1991). Ogilvie et al. suggested that these originated from upward beams of accelerated ionospheric electrons seen at low altitudes (*Sharp et al.*, 1980; *Klumpar and Heikkila*, 1982; *Collin et al.*, 1982; *Burch et al.*, 1983). For adiabatic, scatter free motion, accelerated ionospheric electrons produced in one hemisphere will arrive at the other ionosphere in the loss cone. Thus, unless they are scattered out of the loss cone, the ionosphere in the other hemisphere must also be a source of electrons to produce the observed counterstreaming. Thus if the source of these streams is indeed acceleration of ionospheric

electrons, their bi-directional nature would prove that they were on closed field lines.

The electron counterstreaming is often balanced (i.e. identical in the field parallel and anti-parallel directions, which is often cited as evidence for an ionospheric source, and thus for closed field lines (e.g. *Traver et al.*, 1991). However, this calls for the two independent ionospheric sources to, coincidentally, have equal strengths (in terms of fluxes) and identical characteristics (in terms of distribution functions of the accelerated electrons produced). This may be unlikely, especially near the solstices when one of the sources would be in summer, the other in winter and the ionospheric conditions are different. *Savin et al.* (1997) report an association of ELF waves with these electrons, raising the possibility that they are accelerated by such waves at the magnetopause. This being the case, the electrons could be of either magnetosheath or ionospheric origin but, for the latter, an additional acceleration and/or heating mechanism would be required at low altitudes for them to escape the ionosphere.

Thus an alternative explanation of counterstreaming electrons would place them on open field lines, where the source is the magnetosheath (with slight heating at the magnetopause). The precipitating electrons would then mirror at low altitudes and return upward giving balanced counterstreaming at all pitch angles outside the loss cone.

The AMPTE-UKS observations strongly suggest that the nature of these electron streams changes continuously as the satellite traverses the LLBL, such that the density increases and the temperature decreases as the magnetosheath is approached, the values being almost identical to the magnetosheath immediately adjacent to the boundary (*Hall et al.,* 1991; *Hapgood and Bryant*, 1992; *Lockwood and Hapgood*, 1998). If this is indeed the case, it is very difficult to see how these electrons are of ionospheric origin, as it would require that the acceleration mechanism active on the ionospheric electrons would be able to match

the electron population in the magnetosheath, such that there is no discontinuity across the last closed field line. The analysis of *Lockwood and Hapgood* (1997) explains the mixing of magnetospheric and magnetosheath electron fluxes across the boundary very well, and places the counterstreaming electrons on the most recently opened field lines. This being the case, the bi-directional streaming must arise from the presence of an injected (and slightly heated) sheath population which has travelled directly from the boundary to the satellite, plus a population which was injected slightly earlier and has mirrored at low altitudes and returned to the satellite.

Traver et al. (1991) also report a variation of the bi-directional stream characteristics across the LLBL and observed the "hot" tail of the distribution above 200 eV. They note that LLBL fluxes are enhanced over both sheath and plasma sheet values at these energies and conclude that some electron heating is required if these are to be of sheath origin. They argued that heating of an ionospheric source was more likely. However, recent observations of electron flows across the magnetopause by *Onsager et al.* (2001) show that such heating does indeed occur. Thus the bi-directional electron streams have come to be seen as evidence for open LLBL topology, rather than a closed one.

1-viii. The LLBL and Flux Transfer Events

Flux transfer events (FTEs) were first identified in data from the dayside magnetopause, taken by the ISEE 1 and 2 (*Russell and Elphic*, 1978, 1979) and the HEOS 2 spacecraft (*Haerendel et al.*, 1978). The key defining features of the events are a bipolar oscillation in the boundary normal component of the magnetic field B_N and a rise in the field strength |B| at the event centre. Studies using the nearby ISEE 1 and 2 craft suggested that the dimension of the FTEs normal to the magnetopause was typically of the order of 1 R_E (a mean Earth radius, 1 R_E = 6370 km) (*Saunders et al.*, 1984 a, b). Statistical surveys of the occurrence of these events showed that they are seen predominantly when the

magnetosheath or interplanetary magnetic field points southward (*Berchem and Russell*, 1984; *Rijnbeek et al*., 1984; *Southwood et al.,* 1986; *Kuo et al.*, 1995; *Kawano and Russell*, 1996; 1997), strongly suggesting an association with patchy and transient magnetic reconnection (*Galeev et al.*, 1986). However, seemingly similar events observed closer to the Earth, and so probably deeper in the magnetosphere, show little or no tendency to occur during southward interplanetary magnetic field (IMF) (*Kawano et al.*, 1992; *Borodkova et al.*, 1995; *Sanny et al.*, 1996). Furthermore, *Sibeck and Newell* (1995) questioned the association of magnetospheric FTEs with southward IMF and magnetosheath field orientations, pointing out that if the sheath field was used, it was usually observed later/earlier in the same pass as the FTE and that the sheath field direction was likely to change in the intervening time. In addition, they pointed out that the spatial structure in the interplanetary medium can often result in the IMF orientation, as observed by an upstream satellite, differing from that of the magnetosheath field and that uncertainties in the propagation delay from the IMF monitor to the magnetopause could be important. However, none of these effects would bias the statistical surveys toward southward IMF conditions, and so they do not offer an explanation of the preponderance of southward IMF/sheath field during FTEs.

Lockwood and Hapgood (1998) have applied the successful model of cusp ion steps (*Lockwood and Smith*, 1992; *Lockwood and Davis*, 1996; Lockwood et al., 1998) to an FTE and proved that the event was a transient entry into the open LLBL. Transient LLBL entries into the LLBL were observed by *Skopke et al.* (1981), and also interpreted in terms of LLBL thickenings. However, these events were not accompanied by the classic bipolar boundary-normal field signatures that define an FTE.

The interior of FTEs is a mixture of magnetospheric and magnetosheath plasma (*Thompsen et al.*, 1987, *Farrugia et al.*, 1988; *Lockwood and Hapgood*, 1998) including energetic magnetospheric ions (Scholer et al., 1982b; *Daly et al.*,

1984). An important feature of FTEs is that they are not equilibrium structures, in that there is a total pressure excess (particle plus field) in the event core (*Farrugia et al.*, 1988; *Rijnbeek et al.,* 1987, *Lockwood and Hapgood*, 1998).

The modelling of *Lockwood and Hapgood* (1998) confirmed that the field lines in the core of an FTE are open, as inferred from the ion composition (*Thompsen et al.*, 1987) and ion velocity distributions (*Smith and Owen*, 1992). Lockwood and Hapgood also used a variant of the method by *Lockwood and Smith* (1992) to show that the field lines in the core of an observed event were opened in a pulse of enhanced reconnection rate. The layered structure of the event was shown to be caused by the subsequent reconnection history. Both numerical simulations and analytic theory predict that such a reconnection pulse will cause an excess (unbalanced) total pressure in the core of the event and this will cause the open LLBL to bulge open, driving a bipolar signal as is the signal propagates (*Scholer*, 1989 1988a; b; *Semenov et al.* 1995; 1991).   On the other hand, *Sibeck* (1990) proposed that the excess pressure is not within the LLBL but in the magnetosheath, making the event a ripple of the boundary. Because of the reconnection signatures in the event core, the Sibeck theory requires that reconnection be ongoing, independent of the pressure enhancement. This theory provoked a great deal of discussion about whether the signatures were bulges in the reconnection layer, caused by a reconnection pulse (*Southwood et al.*, 1988; *Scholer*, 1989 1988a; b; *Semenov et al.* 1995; 1991), or corrugations of the reconnection layer, driven by magnetosheath pressure pulses (*Sibeck,* 1992; *Song et al.,* 1994; *Lockwood,* 1991; *Elphic*, 1990). Searches for upstream pressure variations in the solar wind have failed to find events that could act as a source of the required small-scale (of order $1R_E$) sheath pressure variations (*Elphic and Southwood*, 1987; *Elphic et al.*, 1994).

2. Observations

On 14 January 2001, the four Cluster spacecraft approached the magnetopause from the tail lobe, close to the 15:00 MLT meridian. Simultaneous measurements were made using a wide array of ground-based instrumentation. An overview of this pass and of the instrumentation deployed is given by *Opgenoorth et al.* (2001), who also study the intersection of the exterior particle cusp by the Cluster craft at about 13:30 UT. In addition, combined Cluster and ground-based observations of polar cap patches, seen between 08:00 and 09:30 on this day, are discussed by *Lockwood et al.* (2001, this issue). Figure 1 presents and overview of the data recorded by Cluster and EISCAT Svalbard Radar (ESR) between 10:30 and 14:00. Figure 1(a) shows the plasma concentrations seen by the ESR beams pointing at low (30°) elevation along the northward magnetic meridian. Figure 1(b) shows the plasma concentrations along the other ESR beam, aligned with the local magnetic field direction. Figure 1(c) shows the ions seen by the CIS instrument of the Cluster C3 spacecraft: differential energy flux is contoured in an energy-time spectrogram format. Figure 1(d) shows the electrons seen in zone 11 of the HEEA detector (i.e. of electrons moving in the $+Z_{GSE}$ direction) of the PEACE instrument, also on the Cluster spacecraft C3: count-rates are contoured in an energy-time spectrogram format.

In this paper, we concentrate mainly on the data taken between 11:00 and 12:30 which includes close conjunctions of the ESR with the DMSP-F15 satellite and the Cluster spacecraft at about 11:44 and 12:20 UT, respectively (marked by the green and purple dashed lines in figure 1). In this interval, the Cluster craft were observing the dayside magnetospheric population often termed boundary plasma sheet (BPS, e.g. *Newell and Meng*, 1992) with frequent, but brief, excursions into the low latitude boundary layer (LLBL). These are marked by the appearance of low-energy sheath ions and electrons (predominantly at energies below 500 eV) and the partial or complete disappearance of magnetospheric electrons (predominantly at energies above 500 eV), but not of the magnetospheric ions. Clear-cut examples of these LLBL entries are seen around 11:23, 11:37 and

12:52, with a more complex but long-lived example around 12:10. Other short-lived examples are also seen before the cusp convected eastward over the craft at around 13:30 (see *Opgenoorth et al.,* 2001, this issue) and further examples were seen in the interval after the cusp intersection and before the passage of the satellites through the magnetopause (not shown here, *see Opgenoorth et al.,* 2001, this issue).

Figure 1(a) shows that the poleward-pointing ESR beam continued to observe poleward-moving events, as it had during the prior interval of southward IMF (see *Lockwood et al.,* 2001, this issue). The numbering scheme used in figure 1 is a continuation of that used in the previous paper. However, these events were slightly less frequent and migrated poleward at a somewhat lower phase speed that they had earlier (see figure 8 of *Lockwood et al.,* 2001, this issue). Another difference is that these were not, in general, seen by the field-aligned ESR beam (figure 1b). *Blelly et al.* (2001, this issue) have shown that even the event that was seen by the ESR field-aligned beam at around 11:00, does not have the same origin as the events (numbers 20, 21, and 22) seen in the northward-pointing beam. At this time the convection pattern was evolving in a complex way, following the northward turning of the IMF.

Figure 2 is an overview of the magnetic field seen by the FGM instruments on the four Cluster craft on this pass: the four panels give B_x, B_y and B_z in GSE coordinates and |B|. All four craft show identical variations of the timescales of interest here. At the start of the plot at 11:00 $[B_x]_{GSE} > 0$, but this reverses to $[B_x]_{GSE} < 0$ after about 12:00: combined with the plasma data (which show a progression from lobe to mantle to dayside plasma sheet), we interpret this as a motion of the craft from tail-like field lines onto dayside field lines; $[B_Y]_{GSE} < 0$ at all times when Cluster is in the magnetosphere, as expected for the 15 MLT location of the craft; $[B_Z]_{GSE} < 0$ until about 12:05, is approximately zero for 12:05-13:15, and subsequently $[B_Z]_{GSE} > 0$ for the remainder of the time that Cluster is within the magnetosphere. Thus Cluster was initially observing the interior

18

boundary layers LLBL/BPS (i.e. on southward-pointing field lines in the magnetic cusp funnel, half way along the boundary field lines between the exterior magnetopause and middle altitudes). For 12:05-13:15 Cluster was observing the field lines that connect the interior and exterior and interior boundaries ($B_Z \approx 0$), and subsequently the craft observed the exterior magnetopause boundary layers (northward field) where they intersected the exterior cusp at about 13:30 (*Opgenoorth et al.*, 2001, this issue). For the LLBL entry event around 11: 23, studied in this paper in detail, the craft are in the interior boundary layers ($B_Z <$ 0). We also look at an event at around 12:10, when the craft were in the region with $B_Z \approx 0$ and one around 12:53. Within this last event is a pulse of positive B_Z, and this event is when the craft are close to the exterior boundary layers ($B_Z > 0$).

Figure 3 of *Lockwood et al.* (2001, this issue) gives the interplanetary magnetic field seen by the ACE spacecraft on this day. *Opgenoorth et al* (2001) report a very high cross-correlation of the clock angle of the magnetosheath field (in the GSE ZY plane) seen by Cluster, once it had emerged from the magnetosphere after 15:00 UT, with the same angle seen by ACE. The conservation of clock angle across the bow shock reveals a lag of 74 min between ACE and the magnetosheath. *Lockwood et al.* (2001, this issue) have cross correlated magnetic perturbation seen by the IMAGE magnetometer chain before the northward turning and derived a lag between ACE and the ionosphere that fluctuated around 75 min. Given that the propagation delay from the magnetopause to the dayside auroral ionosphere is typically 1-2 mins., these lag estimates are highly consistent. In the interval studied in this paper, the lagged IMF is predominantly northward: the effects of a clear northward turning of the IMF seen by ACE around 09:50 being clearly detected around 11:00 in magnetometer deflections and the transpolar voltage from potential model fits to the SuperDARN radar data. We here concentrate on the Cluster data taken in intervals marked B and C in figure 3 of *Lockwood et al* (2001, this issue). Allowing for the derived propagation lag of 75 min., these intervals correspond to 11:19-11:27 UT and 12:00-12:20 UT, which both have northward IMF (for interval

B, $B_z \approx$ +3nT, $B_y \approx$ +1.5nT in GSM coordinates, giving a clock angle $\theta_{IMF} \approx$ 26° ; for interval C, $B_z \approx$ +3nT, $B_y \approx$ - 3nT, giving $\theta_{IMF} \approx$ 45°). However, both follow intervals in which the IMF B_z component briefly fell to near to zero ($\theta_{IMF} \approx$ 90°), with a positive IMF B_y.

This association is stressed in figure 3 which plots the PEACE electron data from Figure 1(d) with the IMF clock angle in GSM (θ_{IMF}, figure 3b), and the solar wind dynamic pressure data observed by ACE (P_{SW}, figure 3c). The interplanetary data are plotted on a timescale that is lagged by the nominal delay of 75 min., but an additional offset of 16.5 min. has been introduced between the PEACE data and the ACE data plots, making the total lag 91.5 min. This lag gives a good alignment of the event seen by Cluster around 12:10 when Cluster and the ESR were in close conjunction. However, figure 3 also demonstrates that there is a general correspondence of the onset of other LLBL events and increases in the IMF clock angle. There is no correspondence with the solar wind dynamic pressure changes at this or any other lag. The origin of the additional lag of 16.5 min, however, requires explanation before the LLBL events can be associated with the swings of the IMF vector toward the magnetospheric equatorial plane (the rises in θ_{IMF}).

2.2 DMSP-F15 Observations

Figure 4 shows (a) the electrons and (b) the ions, observed by DMSP-F15 as it passed equatorward, moving close to the ESR field-aligned beam around 11:44. The path of the satellite, relative to the two ESR beams, is given in figure 5 in invariant latitude – Magnetic Local Time (Λ-MLT) coordinates. In figure 4, the differential energy flux is plotted as a function of energy (increasing upward) and observation time. The satellite entered the polar cap, passing through an auroral oval showing a series of inverted-V electron arcs at 11:36-11:39 UT, at around Λ = 70° and 19:00 MLT. The purple line in figure 4(c) shows the horizontal

convection velocity perpendicular the satellite track which changed from sunward (meaning from right to left when looking forward along the orbit) to weakly "antisunward" (meaning from left to right across orbit)   close to the poleward edge of this auroral oval. The segment of the DMSP-F15 path that revealed the sunward flow channel and inverted-V events is marked with a thicker line in figure 5. At the poleward edge of the inverted-V events, the satellite observed a convection reversal boundary, with antisunward flow persisting thereafter.

The satellite was then briefly within a region where it observed polar cap precipitation, with brief intersections of magnetosheath. No significant ion flux was seen and the convection was antisunward. This persisted until about 11:41:30, when the satellite began to observe persistent sheath electron fluxes. This segment of the orbit is also marked with a thick line in figure 4, labelled sheath-like electrons because the spectrum is notably lacking the lowest energy electrons of the sheath distribution. At this time, weak fluxes of ions are seen at about 3-20 kV. Just before the satellite's closest conjunction with the field-aligned ESR beam (at around 11:44, orange and black dashed line) the electron spectrum becomes a low-flux, low-energy sheath distribution which persists until the satellite passes through the open-closed boundary (OCB) estimated here to be at 11:45 (red and black dashed line). The OCB is identified by the disappearance of the weak sheath electron population and the onset of persistent BPS electrons. After 11:45 there is a brief dispersed electron event at low energies and a brief drop out of the BPS electrons (at energies above about 1keV). This may be a brief re-encounter with the OCB, but this is not as clear-cut as in the example presented by *Lockwood et al.* (2001, this issue). The OCB location is also marked on Figure 5.

2.3 Convection and Magnetometer Observations

Figure 5 also plots the flow streamlines (equipotentials 5 kV apart) derived by the AMIE technique for 11:40-11:45 UT, when the DMSP-F15 satellite was close to the ESR. The technique has used observations by the SuperDARN radars, ground-based magnetometers, the EISCAT radars and the DMSP satellites. The pattern shows a dominant dusk cell with only a weak dawn cell. The pattern appears to show a convection throat at high latitudes ($\Lambda \approx$ 80-85°) in the morning sector with eastward and poleward flow into the polar cap, suggesting negative IMF B_y (*Heelis et al.,* 1976). However, the lagged IMF data at this time gives positive IMF B_y and such an interpretation would place both the ESR beams on closed field lines, inconsistent with the OCB location deduced from figure 4. This will be discussed again below.

The evolution of the pattern to the form shown in figure 5 is presented in figure 6. At 11:05, the lagged IMF had turned northward, but the convection pattern had yet to respond in any significant way (the transpolar voltage is 55kV, which was the value it had during the prior period of southward IMF (see figure 3, *Lockwood et al.*, this issue), other than a small patch of low flow appeared just to the west noon. The flow pattern had a vigorous dawn cell as well as the dominant dusk cell and the flows in the dayside polar cap were poleward and weakly westward, consistent with the weakly positive IMF B_Y. At 11:10, the transpolar voltage had dropped to 49kV and the slow flow feature evolved into an unusual distortion of the dusk cell around noon. The perturbation to the flow had additional antisunward flow just to the west of the ESR, with additional sunward flow to the west of that. By 11: 15 only the additional poleward flow could be resolved, it having migrated towards dusk, such that it was to the east of the ESR. The transpolar voltage had fallen to 39 kV. At 11:20 the transpolar voltage had risen again to 47 kV, mainly due to a second enhancement in poleward flow, which like the previous one, appears first near noon. The first enhancement in poleward flow can still be defined and has moved further east (but at a slower speed), it being around 16:00 MLT at this time.   After 11:25 the transpolar voltage was roughly constant at a baselevel of about 35 kV. This value is likely to reflect the

rate of open flux destruction in the tail, in which case further enhancements in the dayside voltage are not going to be reflected in the transpolar voltage. It appears that poleward flow features form near noon at 11:10, 11:20 and then migrate east.

This eastward propagation may offer an explanation of some or all of the delay of 16 min between the IMF clock angle changes and the seemingly associated LLBL entry event. A more detailed study of the enhancements at the ESR/IMAGE meridian is presented in figure 7, which shows the 3 components of the lagged IMF data (by the nominal 75 min), the electron data seen by PEACE-C4 (panel d), and the upward continuation of the ground B_x perturbation, B_x', seen by the IMAGE chain, in the same format as used by *Lockwood et al.*(2001, this issue). A positive X (northward) component ($B_x' > 0$) is a response to an eastward current. If the magnetometers are responding to a Hall current in the E-region (i.e. horizontal stratification of conductivities can be assumed) this corresponds to a westward convection velocity in the F-region. Note that the yellow and red colours reveal positive B_x' (eastward current and thus westward flow) whereas green and blue reveal negative B_x' (westward current and thus eastward flow). Between 11:00 and 12:00 (roughly 14:45-15:45 MLT) westward flow was seen poleward of weaker eastward current south of the ESR – only the former of these can be seen in the AMIE flow patterns shown in figure 6. Figure 7e shows clear increases in B_x' a few minutes (respectively about 7 and 5 min) before the first two LLBL entry events at Cluster (at around 11:23 and 11:37 UT – figure 7d), note that the first of these is clear at the highest latitudes but is slightly masked by the (declining) residue of enhanced Bx' due to the southward IMF prior to the northward turning. For these two events, the relevant part of the IMAGE magnetometer chain is at an MLT 49 and 35 min ahead of Cluster. For the third LLBL event around 12:10 there is an almost coincident enhanced B_x' event. In this third case, IMAGE is at essentially the same MLT as Cluster. These data are consistent with events propagating eastward at about 7 min of MLT per min (roughly 0.9 km s^{-1} at ionospheric altitudes) – and giving both the enhanced

flow signatures (detected as B_x' increases) and a transient entry of the Cluster craft into the LLBL.

If these events are also manifest as the poleward flow enhancements near noon seen in figure 6 (that commence in the intervals 11:05-11:10 and 11:15-11:20), they must have moved from noon to the IMAGE meridian at the higher average speed of 14 min of MLT per 1 min (approximately 1.8 km s^{-1}) between 12 MLT and 14 MLT (double the average speed between IMAGE and Cluster at 14 MLT and 15 MLT) . This is consistent with the flow perturbations highlighted in figure 6, as they moving rapidly east initially and then slow down. Thus the first detected signatures of the events seen by Cluster appear to be the flow enhancements near noon at about 11:07:30 and 11:17:30 in the AMIE convection plots. These are both just 5 min after the transient swings of the IMF to near 90-degree clock angle and, allowing for the magnetopause to ionosphere propagation delay of 1-2 min, this is within the uncertainty of the nominal lag estimate of 75 min.

2.4 Cluster Observations

Table 1. Cluster Craft coordinates and separations at 11:23 on 14 January 2001

	C1	C2	C3	C4
X_{GSM} (R_E)	1.7446	1.8096	1.7893	1.7282
Y_{GSM} (R_E)	7.1268	7.0869	7.1706	7.0970
Z_{GSM} (R_E)	8.9529	8.9065	8.8869	8.8689
r (R_E)	11.5754	11.5250	11.5584	11.4896
ϕ_{GSM} (°)	50.6641	50.6060	50.2526	50.5255
θ_{GSM} (°)	76.2452	75.6756	75.9890	76.3138
d_i (R_E)	11.1751	11.1282	11.1734	11.0833
D_{mp} (R_E)	-2.3993	-2.4015	-2.3878	-2.4881

$\Delta_1 X_{GSE}$ (km)	0	414.6287	285.0409	-103.9391
$\Delta_1 Y_{GSE}$ (km)	0	-249.2815	286.1437	-181.0572
$\Delta_1 Z_{GSE}$ (km)	0	-299.7885	-415.2994	-538.0202
$\Delta_1 L$ (km)	0	207.4486	567.3594	258.0507
$\Delta_1 M$ (km)	0	525.1446	96.8506	219.0948
$\Delta_1 N$ (km)	0	15.1349	52.0692	-467.9409
$\Delta_1 r$ (km)	0	-321.1767	-108.1304	-546.2790
$\Delta_1 \phi_{GSM}$ (°)	0	-0.0580	-0.4114	-0.1386
$\Delta_1 \theta_{GSM}$ (°)	0	-0.5696	-0.2562	0.0686
$\Delta_1 d_i$ (km)	0	-298.7955	-10.7349	-584.4671
$\Delta_1 D_{mp}$ (km)	0	-13.5909	73.7636	-565.1925

Figures 8-11 present a detailed analysis of the Cluster data from the interval 11:19 to 11:27 which includes the second of the transient LLBL events shown in figure 1. Table 1 gives the coordinates of the Cluster craft for this interval: the X, Y and Z coordinates in GSM; the geocentric distance ,r; the latitudinal and longitudinal angles, ϕ_{GSM} and θ_{GSM}, respectively; the field-aligned distance to the ionosphere, d_i; and the smallest distance of the craft to the model magnetopause of *Shue et al.* (1997), D_{mp}. All these parameters are also referenced to spacecraft C1, so for example $\Delta_1 X_{GSM}$ is the difference between the X_{GSM} of the craft considered to that of craft 1. Whereas the coordinates are given in Earth radii ($1R_E$ = 6370 km), the separations are given in km. The separations are also given in boundary-normal co-ordinates (L,M,N). The boundary-normal orientation was firstly determined from a model because the craft did not intersect the magnetopause until some considerable time after the events discussed here. However, when it did intersect the magnetopause at around 15:30, the boundary normal coordinates were found by the minimum variance technique to be almost exactly as for this model. We employ the minimum variance results that give unit

vectors of ($\underline{l}$, $\underline{m}$, $\underline{n}$) and ($\underline{i}$, $\underline{j}$, $\underline{k}$) in the boundary normal and GSE frames which are related by $\underline{l}$ = (0.32$\underline{i}$ + 0.59$\underline{j}$ –0.74$\underline{k}$), $\underline{m}$ = (0.63$\underline{i}$ - 0.71$\underline{j}$ -0.29$\underline{k}$), and $\underline{n}$ = (0.70$\underline{i}$ + 0.37$\underline{j}$ +0.61$\underline{k}$). These values are sufficiently accurate to ensure that B_n is relatively small throughout the interval.

Table 1 shows that craft C3 is closest to the model magnetopause (both $\Delta_1 D_{mp}$ and $\Delta_1 N$ are maxima for this craft, equal to, respectively, +73.8km and +52.1 km) whereas C4 is predicted to be the deepest into the magnetosphere (both $\Delta_1 D_{mp}$ and $\Delta_1 D_{mp}$ are minima of -565.2km and –467.9 km); C1 and C2 are at similar distance from the model boundary and $\Delta_1 D_{mp}$ and $\Delta_1 N$ give different answers as to which is closest: $\Delta_1 D_{mp}$ is –13.6 km for C2 whereas $\Delta_1 N$ is +15.13km.

Figure 8 compares the electron and ion data observed by the PEACE and CIS instruments on the 4 craft during this interval. The top four panels show the data from the HEEA detector of PEACE for, from top to bottom, craft C1, C2, C3 and C4. Data are shown for zone 11 which means the electrons are moving in the $+Z_{GSE}$ direction. This zone gives a continuous data series at highest time resolution. The count rates (proportional to differential energy flux) are shown in spectrogram format as a function of energy and time. Also shown are data from the three functioning CIS ion instruments (on board, in order, C1, C3 and C4). The differential energy flux is shown in energy-time spectrogram format, integrated over all pitch angles. The arrows mark the appearance and disappearance of the lowest energy (<100 eV) magnetosheath electrons in the PEACE data. They are reproduced on the CIS data panels are it can be seen that these points also mark the appearance and disappearance of the largest fluxes of magnetosheath ions. However, careful inspection reveals that there are some lower fluxes of sheath ions seen outside of these two arrows, particularly by C1 and C3.

Outside of the arrows, the electron data reveal both a continuously dispersed disappearance and re-appearance of magnetospheric electrons and a similarly dispersed appearance and loss, respectively, of lower energy sheath electrons. This reveals that the spacecraft has passed through a layered structure rather than witnessing a transient loss of magnetospheric electrons (for the latter, the highest energy sphere electrons would have reappeared first and the lowest energy sheath electrons would have disappeared last). This layering is consistent with the satellite passing onto open field lines along which magnetosphere electrons were being lost by flowing out across the magnetopause, and magnetosheath electrons were being gained, by flowing in the opposite direction: the time of flight dispersion of both reveals that the satellites passed onto field lines that had been open for longer at the event centre before returning to closed field lines.

The apparent difficulty for this interpretation are the magnetospheric ions. Figure 8 shows that their flux is not altered much at all in the event, and remains constant, even when the magnetosheath ions are present. This cannot be an effect of the longer flight time of the ions (compared to electrons of the same energy) because the sheath ions have had time to arrive. Data from the RAPID instrument at higher energies in confirms the decrease in flux of magnetospheric electrons but only small reductions in the flux of the ions (Wilken et al., 2001, this issue). Thus, if the satellite is moving onto, and then deeper into, open field lines in this event, some process is maintaining the flux of magnetospheric ions on these newly-opened field lines. The only alternative explanation is that the sheath plasma has been injected onto closed field lines, but this does not explain the loss of the magnetospheric electrons, nor the dispersion ramps outside the arrows.

Figure 9 gives the moments of the ion gas, as observed by the CIS instrument spacecraft 4. The times of the relevant pair of arrows in figure 8 are given by the two vertical lines. The panels show: (a) the proton number density, $N(H^+)$; (b) the

alpha particle number density, $N(He^{++})$; (c) the field-parallel ion temperature, $T_{||}$; (d) the field-perpendicular ion temperature, $T_\perp$; and the ion velocity components (e) V_X, (f) V_Y, and (g) V_Z, in GSE coordinates. The number density of protons and alpha particles show the same waveform, such that the fraction of alpha particles is about 10% throughout. The mixing of the two populations means that the lower temperature sheath plasma depresses the temperatures in the event, in particular the perpendicular temperature which falls from typical magnetospheric values of order 5×10^7 K for this location close to the dayside magnetopause to of order 2×10^6 K in the event centre which is typical of sheath values for this magnetopause location. The number densities confirm that there is additional plasma outside the event boundaries, particularly in its wake, but they have only a small effect on the average temperatures. At the event centre, the velocities are of order $[V_X]_{GSE}$ = -20 km s^{-1}, $[V_Y]_{GSE}$ = 25 km s^{-1} and $[V_Z]_{GSE}$ = - 25 km s^{-1}. Although these point away from noon around the magnetopause, these are much smaller than the values seen once Cluster does emerge through the magnetopause and into the sheath, which average $[V_X, V_Y, V_Z]_{GSE}$ = [-170, 65, -70] km s^{-1} (see below).

These characteristics clearly define the plasma to be the low-latitude boundary layer (LLBL) with a mixture of magnetospheric plasma and magnetosheath plasma, flowing antisunward but at much slower speed than the sheath itself. (*Mozer et al.*, 1994).

The spacecraft potential is measured by the EFW instrument on each craft and varies with the ambient plasma concentration. Figure 10 shows the values for spacecraft C1 (in black), C2 (red), C3 (green) and C4 (blue). All craft see the same variation, with minima outside a main central enhancement where the magnetospheric electrons are lost and magnetosheath plasma are gained, respectively. All satellites see a small secondary peak after the main peak, as can be seen in the N[H$^+$] and N[He^{++}] variations in figure 9. The signatures are nested to some extent, with C4 entering the event last and emerging from it first.

Table 1 shows that C4 is the furthest from the nominal magnetopause location (it has the largest $|D_{mp}|$) and thus this supports the concept of a travelling indentation of the boundary. Nesting is not so clear for the other craft. The order of the observed event durations (from longest to shortest) is C2, C3, C1, C4; whereas the order set by a constant nested signature and the boundary-normal separations $\Delta_1 N$ (see Table 1) would be C3, C2, C1, C4. The arrows in figure 10 are at the same times as those in figure 8: they are colour coded using the same scheme as the graphs. The duration and nesting of the events defined this way are similar to those derived from the EFW spacecraft potential data.

Cross-correlating the signatures seen at the craft gives a phase lag between spacecraft, which can be used to give one estimate of a phase velocity of $[V_X, V_Y, V_Z]_{GSE} = [-24, 0, 9]$ km s^{-1}, which in turn yields $V_{||} = 1$ km s^{-1} and $V_\perp = 26$ km s^{-1} in relation to the average magnetic field direction and $[V_L, V_M, V_N] = [-14.3, -17.7, -11.31]$ km s^{-1} in boundary-normal coordinates. The event is moving antisunward and into the magnetosphere, rather than around its dusk flank. Thus the event demonstrates a field-perpendicular convection of flux tubes, mainly moving in the antisunward (-X) direction. Using the Tsyganenko T96 model with appropriate inputs, this velocity maps to a speed of ionosphere $V_i \approx 0.8$ km s^{-1}, in a direction poleward and away from noon around the afternoon sector. The core of the event at C2 lasts for 210 s, which gives a length of structure, at the magnetopause and in its direction of motion of $L \approx 26 \times 210 = 5460$ km $(\sim 1R_E)$, which mapped to ionosphere gives $L_i \approx 140$ km. Note that the average ion velocities within the event (see figure 9) are comparable in magnitude, but not precisely the same as, the derived event phase motion, but that the phase motion is much lower than the exterior sheath speeds seen after the magnetopause crossing. Average velocities for 5 min after the satellites emerge into the sheath (i.e. for 15:09-15:14 UT) are $[V_X, V_Y, V_Z]_{GSE} = [-170, 65, -70]$ km s^{-1}, giving $[V_L, V_M, V_N] = [35.7, -133.0, -137.7]$ km s^{-1}. The large negative V_N probably indicates that the satellites are already deep into the magnetosheath for much of this time. The best alignment of sheath flow with the nominal boundary

plane is seen at 15:06:10, when $[V_X, V_Y, V_Z]_{GSE}$ = [-80,100, -15] km s^{-1}, giving $[V_L, V_M, V_N]$ = [44.5, -117.1 -28.1] km s^{-1}. For either estimate, the sheath flow velocity is an order of magnitude larger than the event phase velocity. Both the event motion and the sheath flow are towards dusk (negative M component) but the event motion is equatorward (negative L) whereas the sheath flow is poleward (positive L), indicating the magnetic curvature force, as well as the sheath flow, is playing a role in the field line evolution. The tension force must have a strong component in the –L direction, implying a high latitude reconnection site. The large differences between both the magnitude and the direction of the event velocity and the sheath velocity mean that this event is certainly not a boundary indentation caused by a feature propagating around the magnetosphere in the magnetosheath.

Figure 11 shows the magnetic field observations during this event in the boundary-normal frame, using the boundary normal orientation discussed earlier. Figure 11 shows no coherent signal in the boundary normal component, B_n, and certainly no bipolar signature that could be interpreted as an FTE. However, largely due to an increase in the B_m component, there is a weak peak in the field magnitude, |B|. Thus the event appears to be an FTE in all but one respect: it has a dimension of about $1R_E$ in its direction of motion; it is moving antisunward into the polar cap and the motion is field-perpendicular; it contains a mixture of magnetosphere and magnetosheath plasma, it shows an excess of magnetic and ion pressure at its centre. The only feature lacking is the bipolar signature in the boundary-normal field.

Unfortunately, skies over Svalbard were cloudy at the time of this event and thus we could not use auroral imagers to observe any corresponding phase motion in the mid-afternoon auroral ionosphere. However, the skies cleared and such observations were possible for the less-clear cut event around 12:10. These are discussed in the next section. For comparison, figure 12 shows the PEACE and CIS data for this event, in the same format as figure 8. Many of the same

features are observed, but there are differences also. The event lasts longer at all craft, but sheath electron fluxes at the centre of the event are not as strong. There are more complex entries into and exits from the event (in particular, for the exit from the event by C2) possibly implying corrugation and wave activity.

2.5 Auroral Observations

Figure 13 shows a sequence of images taken at 630 nm by the all-sky camera at Ny Ålesund, Svalbard for 12:00-12:34. The images are in geographic frame, with north up the page and lines of constant geographic latitude and longitude marked. Each frame also shows the outline of Svalbard and the east coast of Greenland and the mapped footprint of Cluster as a function of time. The luminosity to the south in each frame is scattered sunlight. Frames are 1-minute integrations, shown every 2 minutes and the luminosity has been mapped by assuming it all arises from 250 km altitude.

At 12:00, there was little 630 nm luminosity along the auroral oval: what there was, can be seen to have been strongest to the west of Svalbard near the east coast of Greenland. The MLT of the observing station at 12:00 is ~14:45 hrs, the western limb of the imager field of view is at an MLT of ~12:15 hrs (for an assumed emission altitude of 250 km). Thus this 630 nm luminosity was in the right location near noon for it to be classed as the cusp aurora. At 12:00 it was mainly to the north of the line denoting the path of the mapped Cluster footprint. By 12:02, this noon cusp aurora had brightened and moved equatorward. Both the brightening and equatorward motion (compare its position relative to the Cluster path) continued until 12:08. This erosion is expected for enhanced reconnection which, allowing for the mean radiative lifetime of the 630 nm emission of 110s plus one minute of time of flight of sufficient ions to allow the electron precipitation flux to become sufficiently large, means a reconnection pulse took place near noon at about 12:00-12:05. Figure 3 shows that with the nominal lag of 75 min., the IMF clock angle was increased in a pulse (during

which it rose above 90º) at 11:54-12:00. Thus this feature appears to be a response to the southward turning of the IMF seen by ACE, but with a lag that is about 5 minutes longer than the nominal value of 75 min. This is certainly within both the uncertainty and the fluctuation level of the lag estimates.

At subsequent times (12:08-12:18) the enhanced aurora spread eastward towards Svalbard. The appearance of a rayed feature to the east of Svalbard At around 12:14 marks its arrival at the zenith of the instrument. Note that this feature is almost certainly exaggerated in size in this and subsequent images because the emission comes from a wide range of altitudes and not just the 250 km (which is near the peak of the volume emission rate) that has been assumed. Given that enhanced luminosity first appears about 2 hours of MLT to the west of Svalbard at 12:02, this is an approximate average propagation speed of 10 min of MLT per min (corresponding to an ionospheric phase speed of 1.3 km s-1, very similar to the initial eastward expansion speeds inferred from the multi-instrument study of the event around 11:23). At subsequent times the cusp aurora continues to brighten and careful inspection reveals fine structure, with a series events propagating poleward and expanding to the east.

Figure 12 shows that the arrival of sheath electrons in the LLBL intersection event began at about 12:07 which, allowing for the particle propagation delay and the radiative lifetime, corresponds to the image at about 12:10. This is about 4 min before the expanding 630 nm aurora reached Svalbard and the Cluster footprint. Given the uncertainties of the field line mapping, it is more than possible that the event seen by Cluster is related to the eastward-expanding 630 nm event. Note that the expansion from first onset at 12:02 to the MLT of the ESR and Cluster (at about 12:14), explains much of the additional 16.5 min lag required to relate the Cluster LLBL entries and the clock angle changes in figure 3.

2.5 Cluster magnetometer observations of an event in the exterior boundary layer

Figure 1 shows that the series of LLBL intersections persists up to the cusp intersection at 13:30, and a particularly clear-cut particle event is seen around 12:53. Figure 14 shows the magnetometer data from the four craft at this time, when Cluster was close to emerging into the exterior boundary layers. Whereas the interior boundary layer events show no clear magnetic signature (figure 11), a signature begins to emerge for this event. Figure 14 shows that this event shows a clear enhancement of the negative B_L in boundary-normal coordinates; 3 of the 4 craft show reduction in the magnitude of the negative B_M and there is a signature in the boundary normal field B_N seen by all craft. The magnitude of the field $|B|$ is increased in a broad peak.

In fact, careful inspection of both the electron and ion data in this event reveals that it was a double event (Figure 1) and this is also seen in figure 14 which shows peaks in $|B_L|$ and $|B|$. In addition, the B_N data reveal two bipolar signatures (with ΔB_N negative then positive) centred on 12:52 and 12:58. Outside of the events, the field is pointing towards dawn and sunward ($[B_x]_{GSE} \approx$ -3nT, $[B_x]_{GSE} \approx$ -20nT, $[B_Z]_{GSE} \approx$ 0) and so the negative the positive polarity signal is consistent with two bumps in the magnetopause propagating antisunward and eastward over the craft. These signatures are thus a pair of FTEs.

3. Discussion and Conclusions

When approaching the magnetopause on an outbound pass on 14 January 2001, Cluster underwent a series of brief intersections with the Low-Latitude Boundary Layer (LLBL), both before and after it intersected the cusp at about 13:30 (*Opgenoorth et al.*, 2001, this issue). These are similar events to those observed

by INTERBALL, as reported by *Savin et al.* (1997), and by GEOTAIL, as reported by *Fujimoto et al*. (1998) but are here observed by the 4 Cluster craft.

The dispersed disappearance and re-appearance of magnetospheric electrons on the edges of these events is consistent with the satellite moving into an open LLBL, as is the appearance of sheath ions. This electron dispersion was also seen in the FTE event studied by *Farrugia et al.* (1988) and modelled by *Lockwood and Hapgood* (1998). However, that event also showed continuous dispersion of ions. The step-like edges of the injected ion events reported here is also consistent with this model, provided the reconnection is pulsed and falls to zero between the pulses (*Lockwood and Davis*, 1996). The two main difficulties with this interpretation are: (1) the maintenance of magnetospheric ions (but not electrons) on the open field lines and (2) the slow convection velocities of the flux tubes. Considering the former, Figure 1(c) shows that some events show slight decreases in magnetospheric ion fluxes, this is clearest for the event around 12:52. The theory of *Cowley* (1982) and modelling by *Lockwood* (1997b) offers an explanation in terms of ions being accelerated on reflection off the Alfvénic disturbances in the reconnection layer (open LLBL), in particular the external RD (Alfvén wave) - the magnetopause - and the faster internal RD. *Lockwood and Moen* (1995) have used ion reflection off the Alfvén waves at an open magnetopause to match the partial moments of LLBL and cusp ions and *Lockwood* (1997a) was able to reproduce the full spin angle distributions. *Lockwood and Hapgood* (1998) used the theory to match the moments and distributions of the ions seen within an FTE.

The remaining difficulty is that the field lines are moving at a velocity that is an order of magnitude slower than the sheath flow, which has been used as evidence for a closed topology (*Fujimoto et al.*, 1998). The presence of sub-Alfvénic ions and electrons means that the field line motion would have responded to the opening of the field lines. Thus for these field lines to be open, we must conclude that the tension force is counteracting the effect of the sheath

flow on the part of the field line that is outside the magnetopause, such that the field lines are hung up on the dusk flank of the magnetosphere.

Table 2 summarises the evidence concerning the key question of the magnetic topology of the field lines within the transient LLBL events. It can be seen that there are problems with either explanation. However, possibilities exist for explaining all features for an open topology, and this is not the case for a closed topology.

The magnetic field measured by FGM in both the magnetosheath and the boundary layer was of order 20nT, but the plasma density seen by CIS was of order, respectively, 10^7 m^{-3} and 2×10^5 m^{-3}. Using the mean ion mass of 1.3 amu seen by CIS on both sides of he boundary (10% He^{++} and 90 % H$^+$), we find that the exterior and interior magnetopause Alfvén waves propagated at speed V_A of order 120 kms^{-1} and 850 kms^{-1}, respectively. Reflection off these waves gives acceleration of ions by up to $2V_A$ (*Cowley*, 1982; *Lockwood et al.*, 1996), which means the peak of the distribution function is shifted to 470 eV for protons (1.88 keV for He^{++}) for the exterior wave and to 23.5 keV (0.94 MeV for He^{++}) for the interior wave. Considering the hot tail of the initial field-parallel magnetospheric distribution, it can be seen that reflection of the interior wave will readily generate MeV ions in the LLBL and cusp, on open field lines, as well as maintaining fluxes of unaccelerated magnetospheric ions on open field lines (*Lockwood*, 1997b).

Comparison of the CIS and PEACE spectrograms at onset of the intersection with the cusp event (13:22-13:27) is identical to the onset of one of the clear-cut the events shown in this paper (e.g. 11:18-11:23). The same is true for the (somewhat protracted) exit from the cusp event. The difference appears to be that in the cusp event the satellite moves onto field lines that have been open long enough for all magnetospheric electrons to vanish and for the low energy ion electron fluxes to rise to about half of the values in the local magnetosheath.

Thus we conclude that the cusp intersection event studied by *Opgenoorth et al*. (2001, this issue) is exactly the same in principle as the events studied here – i.e. newly-opened flux was formed by reconnection in the morning sector and dragged eastward to the satellites in all cases. The only difference is that more open flux was formed in the cusp event than in these LLBL events and they convected further over the Cluster craft so that they sampled field lines of greater elapsed time since reconnection. In the cusp event, as in the LLBL events presented here, an additional propagation lag was required to match the IMF clock angle variations to the event. As for the events studied here, ground-based data reveal that the lag was due to event formation in the pre-noon sector and propagation to the mid-afternoon location of the craft.

Table 2. Summary of explanations of observed features of the LLBL events.

Feature	Explanation for a Closed Topology	Explanation for an Open Topology
1. Appearance of magnetosheath ions	No viable mechanism known	Well explained as ions flowing along open field lines
2. Loss of magnetospheric electrons	Mechanism also unknown, but must act on opposite side of magnetopause to the mechanism invoked to explain 1, yet be active at the same time and place	Well explained by electrons flowing along open field lines
3. Sharp edges to sheath ion regions	Not known	Requires reconnection pulses
4. Dispersed loss of electrons	Not known	Well explained by time of flight of escaping electrons

5. Maintenance of magnetospheric ions	Well explained	Requires ion reflection off magnetopause Alfvén waves or a magnetic bottle on open field lines
6. Some weak loss of magnetospheric ions in some events	Not explained	Requires only a weakening of the mechanism invoked for 5.
7. Low event phase velocity (and similarly low field-perpendicular plasma velocity within event)	Consistent	Requires geometry such that tension force and sheath flow are close to being in balance
8. Balanced counterstreaming electrons	Requires identical electron acceleration in both ionospheres (even if there is additional heating at the magnetopause)	Requires weak heating of entering sheath electrons at magnetopause (which then mirror at low altitudes)
9. Correspondence with IMF clock angle	Not explained	Well explained as reconnection pulses
10. No correspondence with solar wind pressure pulses	Eliminates for several suggested mechanisms	Consistent
11. Ionospheric events	Not explained	Well explained as reconnection pulses

The events take place during predominantly northward IMF and appear to be triggered by swings of the IMF towards the ecliptic so that the IMF clock angle approaches 90 degrees in GSM coordinates. However, the lag is 15-20 min longer than observed both before and after the period of interest here. The ground-based observations explain this additional delay because signatures in both the flows and in the 630 nm aurora indicate that the events form in the pre-noon sector and most of the additional delay is the time taken for the events to propagate eastward to the mid-afternoon sector. The speed of eastward phase motion see by the ground-based instruments (of order 1 km s^{-1}) is consistent with the phase motion of the event derived from multi-craft studies using Cluster. The propagation of active segments of reconnection X-lines away from noon was first inferred from EISCAT radar data by *Lockwood et al.* (1993) and sketched schematically by *Lockwood* (1994). *Lockwood et al.* (1995) used this concept to show that FTEs can be responsible for the full transpolar voltage. Recently, *Milan et al.* (2000) has found further evidence for this concept in HF coherent radar data and UV global images: it has also been used to explain multi-instrument and multi-point data by *McWilliams et al.* (2001).

The occurrence of these events is consistent with the idea that "subsolar" reconnection (meaning the production of open field lines by the merging of closed field lines and draped interplanetary field lines, which may take place away from the equatorial plane) persists when the IMF is northward, at least as long as the IMF clock angle is greater than about 45°. The direction of motion of the event is in the –L direction (equatorward) whereas the local sheath flow is positive, suggesting the magnetic curvature force has an equatorward component and that the reconnection site responsible for the reconnection pulse was at high latitudes.

The ESR observed poleward-moving events which are also thought to be reconnection pulse signatures. The lower occurrence rate of events, compared to the earlier interval of southward IMF (*Lockwood et al.*, 2001, this issue) is

consistent with the triggering of the northward IMF events by swings of the IMF to greater clock angle. The events were not, in general, seen by the field-aligned ESR beam. For much of the period this may be because that beam was equatorward of the open-closed boundary. However, this was not the case during the pass of the DMSP-F15 satellite just after one of the events and not long after the northward turning. This revealed the ESR field-aligned beam to be on open field lines. However, these were "old" open field lines for which the magnetopause threading point was a long way down the tail and hence sheath precipitation fluxes were low. The newer open field lines were seen as a region of higher sheath fluxes that were to the dusk side and not near noon. We can identify this patch of sheath plasma precipitation with one of the poleward-moving enhancements seen by the low elevation ESR beam.

Given that these events are well explained as transient plasma injections caused by bursts of reconnection, the one major surprise is that there was no bipolar deflection in the field, at least in most of the cases. This is the classic characteristic used to define FTEs. However, it is important to remember where these Cluster observations were made. Most of the events were seen on southward-pointing field lines, i.e. on the boundary of the interior magnetic cusp, half way between the magnetopause boundary layer and its projection at middle altitudes. Only the last events, for which the satellites were moving onto northward pointing field, showed indications of bipolar FTE field signatures. Even in these cases, the bipolar signature was weak; however, we note that B_z was still close to zero and thus the satellites were only just entering the exterior boundary layer. We conclude that the bipolar FTE signatures are a feature only of the exterior boundary layer. They are not seen on the southward-pointing field on the edges of the interior magnetic cusp (as, indeed, nor are they seen at middle altitudes).

The lack of a bipolar magnetic signature for the first event studied here (at around 11:23) is because the event does not bulge out in response to increased

pressure within the event. The magnetic field magnitude (pressure) is of order 30 nT (0.36 nPa) in the event centre and 24 nT (0.23 nPa) outside it. Thus the field pressure excess for this event is 1.3 nPa. Figure 9 shows that the ion concentration, parallel temperature and perpendicular temperatures at the event centre are of order 6.31×10^5 m^{-3}, 2.51×10^7 K and 3.16×10^6 K, respectively. The corresponding values outside the event are 2.00×10^5 m^{-3}, 6.31×10^7 K and 6.31×10^7 K. These numbers yield a roughly isotropic ion pressure outside the event of 0.17 nPa, but field-perpendicular and field-parallel ion pressures of 0.03Pa and 0.22 nPa inside it. Thus the drop in field-perpendicular ion pressure was 0.14 nPa and there was a slight rise in the field-parallel ion pressure of 0.05nPa. Full pressure balance considerations (including the electron gas) will be made elsewhere, but we note that the increased magnetic pressure in this event is comparable with the drop in field-perpendicular ion pressure. Thus these events are much closer to being in pressure equilibrium than are the FTEs on the exterior boundary: this being the case, a bipolar magnetic signature is not expected.

This can be contrasted with the event closer to the outer boundary around 12:50 (for which a bipolar magnetic FTE signature was seen). In this event, the field magnitude rose from 20 to 24 nT, giving a modest field pressure increase of 0.04 nPa. The ion concentration variation was similar to the 11:23 case, but the perpendicular temperature fell to only 3×10^7 K, such that the ion pressure rose from 0.17 nPa outside the event to 0.25 nPa inside it. Thus both the magnetic and ion pressures show an excess in this event, consistent with the bipolar field signature and with FTE events on the exterior magnetopause boundary.

References

Akasofu, S.I., E.W. Hones, Jr., S.J. Bame, J.R. Ashbridge, and A.T.Y. Lui, Magnetotail and boundary layer plasma at geocentric distance of 18 R$_E$, *J. Geophys., Res., 78*, 7257, 1973.

Alem, F., and D.C. Delcourt, Nonadiabatic precipitation of ions at the cusp equatorward edge, *J. Geophys. Res., 100*, 19,321, 1995.

Anderson, B.J., T.D. Phan, and S.A. Fuselier, Relationships between plasma depletion and subsolar reconnection, *J. Geophys. Res., 102,* 9531-9542, 1997.

Aparicio, B., B. Thelin, and R. Lundin, The polar cusp from a particle point of view: A statistical model based on Viking data, *J. Geophys. Res.,* 14,023, 1991.

Berchem, J., and C. T. Russell, Flux transfer events on the magnetopause: Spatial distribution and controlling factors, *J. Geophys. Res., 89*, 6689-6703, 1984.

Bodokova, N.L., G.N. Zastenker and D.G. Sibeck, A case and statistical study of transient magnetic field events at geosynchronous orbit and their solar wind, *J. Geophys. Res.,* **100**, 5643-5656, 1995.

Boyle, C.B., P.H. Reiff, and M.R. Hairston, Empirical polar cap potentials*, J. Geophys. Res., 102*, 111-125, 1997.

Burch, J. L., Quasi-neutrality in the polar cusp, *Geophys. Res. Lett., 12,* 469-472, 1985

Burch, J.L., P.H. Reiff and M. Sugiura, Upward electron beams measured by DE-1: a primary source of dayside region 1 Birkeland currents, *Geophys. Res. Lett., 10,* 753-756, 1983.

Chandler, M.O. , S.A. Fuselier, M. Lockwood and T.E. Moore, Evidence of component magnetic merging equatorward of the cusp , *J. Geophys. Res., 104* , 22623-22648, 1999

Collin, H.L., R.D. Sharp and E.G. Shelley, The occurrence and characteristics of electron beams over the polar regions, *J. Geophys. Res., 87,* 7504, 1982.

Cowley, S.W.H., The causes of convection in the Earth's magnetosphere: A review of developments during IMS, *Rev. Geophys., 20*, 531-565, 1982.

Cowley, S.W.H., Solar wind control of magnetospheric convection, in *Achievements of the international magnetospheric study, IMS*, pp 483-494, ESA SP-217, ESTEC, Noordwijk, The Netherlands, 1984.

Cowley, S.W.H., and Z.V. Lewis, Magnetic trapping of energetic particles on open dayside boundary layer flux tubes, *Planet. Space Sci., 38*, 1343, 1990.

Cowley, S.W.H., M.P. Freeman, M. Lockwood and M.F. Smith, The ionospheric signature of flux transfer events*, in "CLUSTER - dayside polar cusp", ed. C.I. Barron, ESA SP-330,* 105-112, European Space Agency Publications, Nordvijk, The Netherlands, 1991

Crooker, N.U., Reverse convection, *J. Geophys. Res., 97,* 19363-19372, 1992.

Daly, P.W., and T.A. Fritz, Trapped electron distributions on open field lines, *J. Geophys. Res., 87*, 6081, 1982.

Daly, P. W., M. A. Saunders, R. P. Rijnbeek, N. Sckopke, and C. T. Russell, The distribution of reconnection geometry in flux transfer events using energetic ion, plasma, and magnetic data, *J. Geophys. Res., 89*, 3843, 1984.

Drakou, E., B.U.O. Sonnercup and W. Lotko, Self-consistent steady state model of the low-latitude boundary layer, *J. Geophys. Res*., **99**, 2351-2364, 1994.

Eastman, T.E., and E.W. Hones Jr., Characteristics of the magnetospheric boundary layer as observed by IMP - 6, *J. Geophys. Res., 84,* 2109, 1979.

Eastman, T.E., E.W. Hones Jr., S.J. Bame, and J.R. Ashbridge, The magnetospheric boundary layer: Site of plasma, momentum and energy transfer from the magnetosheath to the magnetosphere, *Geophys. Res. Lett.*, 3, 685-688, 1976.

Elphic, R. C., Observations of flux transfer events: Are FTEs flux ropes, islands, or surface waves?, in *Physics of Magnetic Flux Ropes*, *Geophys. Monogr.*

Ser., vol. 58, edited by C. T. Russell, E. R. Preist, and L. C. Lee, pp. 455-472, AGU, Washington, D. C., 1990.

Elphic, R.C., and D.J. Southwood, Simultaneous measurements of the magnetopause and flux transfer events at widely separated sites by AMPTE UKS and ISEE 1 and 2, *J. Geophys. Res., 92,* 13,666-13,672, 1987.

Elphic, R. C., M. Lockwood, S. W. H. Cowley, and P. E. Sandholt, Signatures of flux transfer events at the dayside magnetopause and in the ionosphere: Combined ISEE, EISCAT and optical observations, *Geophys. Res. Lett., 17,* 2241-2244, 1990.

Elphic, R.C., W. Baumjohann, C.A. Cattell, H. Lühr, and M.F. Smith, A search for upstream pressure pulses associated with flux transfer events: An AMPTE/ISEE case study, *J. Geophys. Res.*, *99*, 13,521-13,527, 1994.

Farrugia, C. J., et al., A multi-instrument study of flux transfer event structure, J. Geophys. Res., 93, 14465-14477, 1988.

Fedorov, A., E. Budnik, M. Novrachev, V. Romanov, P. Song, J.-A. Savaud, Plasma characteristics near the exterior cusp under different orientations of the interplanetary magnetic field, *Czech J. Phys., 49*, 711-732, 1999

Freeman, M.P., C.J. Farrugia, L.F. Burlaga, M.R. Hairston, M.E. Greenspan, J.M. Ruohoniemi, and R.P. Lepping, The interaction of a magnetic cloud with the earth: ionospheric convection in the northern and southern hemispheres for a wide range of quasi-steady interplanetary magnetic field conditions, *J. Geophys. Res., 98,* 7633-7655, 1993.

Fujimoto, M., T. Terasawa, T. Mukai, Y. Saito, T. Yamamoto, and S. Kokubun, Plasma entry into the flanks of the near-Earth magnetotail: Geotail observations, *J. Geophys. Res., 103*, 4391-4408, 1998

Fuselier, S.A., D.M. Klumpar, and E.G. Shelley, Ion reflection and transmission during reconnection at the Earth's subsolar magnetopause, *Geophys. Res. Lett., 18,* 139, 1991

Fuselier, S.A., D.M. Klumpar, and E.G. Shelley, Counter-streaming magnetosheath ions in the dayside low latitude boundary layer, *Geophys. Res. Lett., 19,* 425-428, 1992

Fuselier, S., B.J. Anderson, and T,G, Onsager, Electron and ion signatures of field line topology at the low shear magnetopause, *J. Geophys. Res.,100,* 11805-11814, 1995.

Fuselier, S.A. , M. Lockwood, T.G. Onsager and W.K. Peterson, The source population for the cusp and cleft/LLBL for southward IMF, *Geophys. Res. Lett., 26,* 1665-1669, 1999.

Galeev, A.A., M.M. Kuznetsova, and L.M. Zeleny, Magnetopause stability threshold for patchy reconnection, *Space Sci Rev., 44*, 1-41, 1986

Gosling, J.T., M.F. Thomsen, S.J. Bame, R.C. Elphic and C.T. Russell, Plasma flow reversals at the dayside magnetopause and the origin of asymmetric polar cap convection, *J. Geophys. Res., 95,* 8073-8084. 1990a.

Gosling, J.T., M.F. Thomsen, S.J. Bame, R.C. Elphic and C.T. Russell, Cold ion beams in the low-latitude boundary layer during accelerated flow events, *Geophys. Res. Lett., 17,* 2245-2248, 1990b.

Gosling, J.T., M.F. Thomsen, S.J. Bame, T.G. Onsager and C.T. Russell, The electron edge of the low-latitude boundary layer during accelerated flow events, *Geophys. Res. Lett., 17,* 1833-1836, 1990c.

Gosling, J. T, M. F. Thomsen, S. J. Bame, R. C. Elphic, and C. T. Russell, Observations of reconnection of interplanetary and lobe magnetic field lines at the latitude magnetopause., *J. Geophys. Res., 96,* 14097-14106, 1991.

Haerendel, G., G. Paschmann, N. Sckopke, H. Rosenbauer, and P. C. Hedgecock, The frontside boundary layer of the magnetopause and the problem of reconnection, *J. Geophys. Res., 83,* 3195-3216, 1978.

Hall, D.S. C.P. Chanelor, D.A. Bryant, D.R. Lepine and V.P. Tritakis, Electrons in the boundary layers near the dayside magnetopause, *J. Geophys. Res., 96*, 7869, 1991

Hapgood, M.A. and D.A. Bryant, Re-ordered electron data in the low-latitude boundary layer, Geophys. Res. Lett. 17, 2043-2046, 1990.

Hapgood, M.A. and D.A. Bryant, Exploring the magnetospheric boundary layer, *Planet. Space Sci., 40,* 1431-1459, 1992.

Hapgood, M.A., and M. Lockwood, On the voltage and distance across the low latitude boundary layer, *Geophys. Res. Lett.,* **20,** 145-148, 1993.

Hapgood, M.A. and M. Lockwood, Rapid changes in LLBL thickness, *Geophys. Res. Lett.,* **22**, 77-80, 1995.

Heelis, R.A., W.B. Hanson, and J.L. Burch, Ion convection reversals in the dayside cleft, *J. Geophys. Res., 81,*3803, 1976.

Heyn, M.F., H.K. Biernat, R.P. Rijnbeek, and V.S. Semenov, The structure of reconnection layers, *J. Plasma Phys., 40(2),* 235-252, 1988.

Hill, T.W., and P.H. Reiff, Evidence of magnetospheric cusp proton acceleration by magnetic merging at the dayside magnetopause, *J. Geophys. Res., 82,* 3623, 1977.

Hones, E.W., Jr., J.R. Ashbridge, S.J. Bame, M.D. Montgomery, S. Singer, and S.-I. Akasofu, Measurements of magnetotail plasma flow made with Vela 4B, *J. Geophys. Res., 77,* 5503, 1972.

Johnstone, A.D., D.J. Rodgers, A.J. Coates, M.F. Smith and D.J. Southwood, Ion acceleration during steady-state reconnection at the dayside magnetopause, in *Ion acceleration in the magnetosphere and ionosphere*, ed. T. Chang, AGU Monograph 38, 136-145, 1986.

Jørgensen, T.S., E. Friis-Christiansen, V.B. Wickwar, J.D. Kelly, C.R. Clauer, and P.M. Banks, On the reversal from "sunward" to "antisunward" plasma convection in the dayside high latitude ionosphere, *Geophys. Res. Lett., I,* 887-890, 1984.

Karlson, K.A., M. Øieroset, J. Moen and P.E. Sandholt, A statistical study of flux transfer event signatures in the dayside aurora: the IMF B_y-related postnoon-prenoon asymmetry, J Geophys. Res., 101, 59-68, 1996.

Kawano, H., and C.T. Russell, Survey of flux transfer events observed with the ISEE spacecraft: rotational polarity and the source region, *J. Geophys. Res., 101*, 27299-27308, 1996

Kawano, H., and C.T. Russell, Survey of flux transfer events observed with the ISEE spacecraft: dependence on the interplanetary magnetic field*, J. Geophys. Res., 102*, 11307-11313, 1997

Kawano, H., S. Kokubun, and K. Takahashi, Survey of transient magnetic field events in the dayside magnetosphere, *J. Geophys. Res., 97,* 10,677-10,692, 1992.

Klumpar, D.M. and W.J. Heikkila, Electrons in the ionospheric source cone: evidence for runaway electrons as carriers of downward Birkeland currents, *Geophys. Res. Lett., 9,* 873, 1992.

Kremser, G., J. Woch, K. Mursala, P. Tanskanen, B. Wilken, and R. Lundin, Origin of energetic ions in the polar cusp inferred from ion composition measurements by the Viking satellite, *Ann. Geophys., 13,* 595-607, 1995.

Kuo, H., C.T. Russell and G. Le., Statistical studies of flux transfer events, *J. Geophys. Res*., **100**, 3513-3519, 1995.

Levy, R., H.E. Petschek, and G.L. Siscoe, Aerodynamic aspects of magnetospheric flow, *AIAA J., 2,* 2065, 1964.

Lin, Y., and L.C. Lee, The structure of reconnection layers in the magnetosphere, *Space Sci. Rev., 65*, 59-179, 1993

Lockwood, M., Flux transfer events at the dayside magnetopause: Transient reconnection or magnetosheath pressure pulses?, *J. Geophys. Res., 96,* 5497-5509, 1991.

Lockwood, M., Ionospheric signatures of pulsed magnetopause reconnection, *in "Physical signatures of magnetopause boundary layer Processes", ed. J.A. Holtet and A. Egeland, NATO ASI Series C, Vol. 425*, Kluwer, 229-243, 1994.

Lockwood, M., The location and characteristics of the reconnection X-line deduced from low-altitude satellite and ground-based observations, 1, Theory, *J. Geophys. Res., 100*, 21,791, 1995

Lockwood, M., The relationship of dayside auroral precipitations to the open-closed separatrix and the pattern of convective flow, *J. Geophys. Res., 102*, 17475-17487, 1997a

Lockwood, M., Energy and pitch angle dispersions of LLBL/cusp ions seen at middle altitudes: predictions by the open magnetosphere model, *Annales Geophys., 15 ,* 1501-1511, 1997b

Lockwood, M., and C.J. Davis, On the longitudinal extent of magnetopause reconnection bursts, *Annales Geophys., 14*, 865-878, 1996.

Lockwood and M.A. Hapgood, How the Magnetopause Transition Parameter Works, *Geophys. Res. Lett., 24*, 373-376, 1997

Lockwood, M., and M.A. Hapgood, On the Cause of a Magnetospheric Flux Transfer Event, *Geophys. Res., 103*, 26453-26478, 1998

Lockwood, M., and J. Moen, Ion populations on open field lines within the low-latitude boundary layer: theory and observations during a dayside transient event*, Geophys. Res. Lett., 23*, 2895-2898, 1996.

Lockwood, M., and J. Moen, Reconfiguration and closure of lobe flux by reconnection during northward IMF: evidence for signatures in cusp/cleft auroral emissions, *Annales Geophys.*, 17, 996-1011, 1999

Lockwood, M., and M.F. Smith, The variation of reconnection rate at the dayside magnetopause and cusp ion precipitation, *J. Geophys. Res., 97,* 14,841, 1992.

Lockwood, M., and M.F. Smith, Comment on "Mapping the dayside ionosphere to the magnetosphere according to particle precipitation characteristics" by Newell and Meng, *Geophys. Res. Lett., 20,* 1739-1740, 1993.

Lockwood, M., and M.F. Smith, Low and middle-altitude cusp particle signatures for general magnetopause reconnection rate variations, I, Theory, *J. Geophys. Res., 99*, 8531, 1994.

Lockwood, M., J. Moen, S.W.H. Cowley, A.D. Farmer, U.P. Løvhaug, H. Lühr and V.N. Davda, Variability of dayside convection and motions of the cusp/cleft aurora*, Geophys. Res. Lett., 20,* 1011-1014, 1993

Lockwood, M.,T.G. Onsager, C.J. Davis, M.F. Smith, and W.F Denig, The characteristics of the magnetopause reconnection X-line deduced from low-altitude satellite observations of cusp ions, *Geophys. Res. Lett., 21*, 2757-2760, 1994.

Lockwood, M., S.W.H. Cowley, M.F. Smith, R.P. Rijnbeek and R.C. Elphic, The contribution of flux transfer events to convection, *Geophys. Res. Lett.* **22**, 1185-1188, 1995

Lockwood, M., S.W.H. Cowley, and T.G. Onsager, Ion acceleration at both the interior and exterior Alfvén waves associated with the magnetopause reconnection site: signatures in cusp precipitation, *J. Geophys. Res., 101*, 21,501, 1996.

Lockwood, M., C.J. Davis, T.G. Onsager, and J.A. Scudder, Modelling signatures of pulsed magnetopause reconnection in cusp ion dispersion signatures seen at middle altitudes*, Geophys. Res. Lett.*, *25*, 591-594, 1998.

Lockwood, M., H. Opgenoorth, A.P. van Eyken, A. Fazakerley, J.-M. Bosqued, W. Denig, J. Wild, C. Cully, R. Greenwald, G. Lu, O. Amm, H. Frey, A. Strømme, P. Prikryl, M.A. Hapgood, M.N. Wild, R. Stamper, M. Taylor, I. McCrea, K. Kauristie, T. Pulkkinen, F. Pitout, A. Balogh, M. Dunlop, H. Rème, R. Behlke, T. Hansen, G. Provan, P. Eglitis, S.K. Morley, D. Alcayde, P.-L. Blelly, J. Moen, E. Donovan, M. Engebretson, M. Lester, J. Waterman, M.F. Marcucci, Coordinated Cluster, ground-based instrumentation and low-altitude satellite observations of transient poleward-moving events in the ionosphere and in the tail lobe, *Annales Geophys*., this issue, 2001

Lotko, W., and B.U.Ö. Sonnerup, The low-latitude boundary layer on closed field lines, in *Physics of the Magnetopause*, *Geophys. Monogr. Ser.,* vol. 90, edited P. Song, B.U.Ö. Sonnerup, and M. Thomsen, pp. 371-383, AGU Washington, D.C., 1995.

Lu, G., A.D. Richmond, B.A. Emery, P.H. Reiff, O de la Beaujardiere, F.J. Rich, W.F. Denig, H.W. Kroehl, L.R. Lyons, J.M. Ruohoniemi, E. Friis-Christensen, H. Opgenoorth, M.A.L. Persson, R.P. Lepping, A.S. Rodger, T. Hughes, A. McEwin, S. Dennis, R. Morris, G. Burns and L Tomlinson, Interhemispheric asymmetry of the high-latitude ionospheric convection pattern, *J. Geophys. Res*., *99,* 6491-6510, 1994.

Lyons, L.R., M. Schulz, D.C. Pridmore-Brown, and J.L. Roeder, Low-latitude boundary layer near noon: An open field line, *J. Geophys. Res*., 99, 2227, 1994.

Manuel, J.R. and J.C. Samson, The spatial development of the low-latitude boundary layer, *J. Geophys. Res*., **98**, 17,367-17,385, 1993.

McCrea, I.W., M. Lockwood, J. Moen, F.Pitout, P.Eglitis and A.D. Aylward, ESR and EISCAT observations of the response of the cusp and cleft to IMF orientation changes, *Annales Geophys.*, *18,* 1009-1026, 2000.

McWilliams, K. A., T.K Yeoman, and G. Provan, A statistical survey of dayside pulsed ionospheric flows as seen by the CUTLASS Finland HF radar, *Annales Geophys.*, 18, 445-453, 2000

McWilliams**,** K.A., T.K. Yeoman, and S.W.H. Cowley, Two-dimensional electric field measurement in the ionospheric footprint of a flux transfer event, 18, *Ann. Geophys.*, 1584-1598, 2001

Milan, S.E., M. Lester, S.W.H. Cowley, and M. Brittnacher, Convection and auroral response to a southward turning of the IMF: Polar UVI, CUTLASS and IMAGE signatures of transient magnetic flux transfer at the magnetopause, *J. Geophys. Res., 105,* 15,741-15,757, 2000.

Mitchell, D.G., F. Kutchko, D.J. Williams, T.E. Eastman, L.A. Frank and C.T. Russell, An extended study of the low-latitude boundary layer on the dawn and the dusk flanks on the magnetosphere, *J. Geophys. Res., 92*, 7394, 1987.

Moen, J., D. Evans, H.C. Carlson and M. Lockwood, Dayside moving auroral transients related to LLBL dynamics*, Geophys. Res. Lett., 23*, 3247-3250, 1996

Mozer, F.S., H. Hayakawa, S. Kokubun, M. Nakamura, T. Okada, T. Yamamoto and K. Truruda, The morningside low-latitude boundary layer as determined from electric and magnetic field measurements on Geotail, *Geophys. Res. Lett*. **21**, 2983-2986, 1994.

Neudegg, D.A., T.K. Yeoman, S.W.H. Cowley, G. Provan, G. Haerendel, W. Baumjohann, U. Auster, K.-H. Fornacon, E. Georgescu, and C.J. Owen, A flux transfer event observed at the magnetopause by the equator-S spacecraft and in the ionosphere by the CUTLASS HF radar, *Annales Geophys., 17*, 707-711, 1999.

Newell, P. T. and C. I. Meng, The cusp and the cleft/LLBL: Low altitude identification and statistical local time variation, *J. Geophys. Res., 93,* 14,549, 1988.

Newell, P.T. and C.-I. Meng, On quantifying the distinctions between the cusp and the cleft/LLBL, in *Electromagnetic coupling in the polar clefts and caps* NATO ASI Ser C, vol. 278, ed. P.E. Sandholt and A. Egeland, pp.87-101, Kluwer Academic Publishers, Dordrecht, 1989.

Newell, P.T., and C.-I. Meng, Mapping the dayside ionosphere to the magnetosphere according to particle precipitation characteristics, *Geophys. Res. Lett., 19,* 609-612, 1992.

Newell, P.T., and C.-I. Meng, Reply, *Geophys. Res. Lett., 20,* 1741-1742, 1993.

Newell, P.T., and C.-I. Meng, Ionospheric projections of magnetospheric regions under low and high solar wind pressure conditions, *J. Geophys. Res.*, *99*, 273, 1994a

Newell, P.T., and C.-I. Meng, Comment on "Unexpected features of the ion precipitation in the so-called cleft/low latitude boundary layer region: Association with sunward convection and occurrence on open field lines" by A. Nishida, T. Mukai, H. Hayakawa, A. Matsuoka, K. Tsuruda, N. Kaya, and H. Fukunishi, *J. Geophys. Res.*, *99*, 19,609, 1994b.

Newell. P.T. and C.-I. Meng, Open and closed low-latitude boundary layer, in *"Polar Cap Boundary Phenomena", ed. J. Moen, A. Egeland and M. Lockwood, NATO ASI Series C,* Kluwer, 1997.

Newell, P.T., W.J. Burke, E.R. Sanchez, C.-I. Meng, M.E. Greenspan, and C.R. Clauer, The low-latitude boundary and the boundary plasma sheet at low altitude: Prenoon precipitation regions and convection reversal boundaries, *J. Geophys. Res., 96,* 21,013, 1991

Nishida, A., Can random reconnection on the magnetopause produce the low-latitude boundary layer?, *Geophys. Res. Lett., 16,* 227-230, 1989.

Nishida, A., and T. Mukai, Reply to comment on "Unexpected features of the ion precipitation in the so-called cleft/low-latitude boundary layer region" by A. Nishida et al., *J. Geophys. Res.*, *99*, 23,367, 1994.

Nishida, A., T. Mukai, H. Hayakawa, A. Matsuoka, and K. Tsuruda, Unexpected features of the ion precipitation in the so-called cleft/low-latitude

boundary layer region: Association with sunward convection and occurrence on open field lines, *J. Geophys. Res., 98,* 11,161, 1993.

Nishida, A., T. Mukai, T. Yamamoto, S. Kokubun and K. Maezawa, A Unified model of the magnetotail convection in geomagnetically quiet and active times, *J. Geophys. Res., 103*, 4409-4418, 1998

Ogilvie, K., R.J. Fitzenreiter and J.D. Scudder, Observations of electron beams in the low-latitude boundary layer, J. Geophys. Res., **89**, 10723, 1984.

Onsager, T.G., A quantitative model of magnetosheath plasma in the low-latitude boundary layer, cusp and mantle *in "Physical signatures of magnetopause boundary layer Processes", ed. J.A. Holtet and A. Egeland, NATO ASI Series C, Vol. 425*, Kluwer, 385-400, 1994.

Onsager, T. G., and S. A. Fuselier, The location of the magnetopause reconnection for northward and southward interplanetary magnetic field, in *Solar System Plasmas in Space and Time, Geophys. Mono. Ser.*, vol. 84, edited by J. L. Burch and J. H. Waite Jr., pp. 183-197, AGU, Washington D. C., 1994.

Onsager, T.G. and M. Lockwood, High-latitude particle precipitation and its relationship to magnetospheric source regions, *Space Sci. Rev., 80,* 77-107, 1997.

Onsager, T. G., C. A. Kletzing, J. B. Austin, and H. MacKiernan, Model of magnetosheath plasma in the magnetosphere: Cusp and mantle precipitations at low altitudes, *Geophys. Res. Lett., 20,* 479-482, 1993.

Opgennoorth, H.J et al., *Annales Geophys*, this issue, 2001

Owen, C.J. and S.W.H. Cowley, Heikkila's mechanism for impulsive plasma transport through the magnetopause: A re-examination, *J. Geophys. Res., 96,* 5565-5574, 1991.

Owen, C.J. and J.A. Slavin, Viscously driven plasma flows in the deep geomagnetic tail, *Geophys. Res. Lett., 19,* 1443-1446, 1992.

Paschmann, G., B.U.Ö. Sonnerup, I. Papamastorakis, N. Sckopke, G. Haerendel, S.J. Bame, J.R. Asbridge, J.T. Gosling, C.T. Russell and R.C. Elphic, Plasma acceleration at the Earth's magnetopause: Evidence for reconnection, *Nature, 282,* 243-246, 1979.

Paschmann, G., I. Papamastorakis, W. Baumjohann, N. Sckopke, C.W. Carlson, B.U.Ö. Sonnerup, and H, Lühr, The magnetopause for large magnetic shear: AMPTE/IRM observations, *J. Geophys. Res., 91,* 11099-11115, 1986.

Paschmann, G., B.U.Ö. Sonnerup, I. Papamastorakis, W. Baumjohann, N. Sckopke, and H, Lühr, The magnetopause and boundary layer for small magnetic shear: convection electric fields and reconnection, *Geophys. Res. Lett., 17,* 1829-1832, 1990.

Phan, T.D., et al., Low-latitude flank magnetosheath, magnetopause and boundary layer for low magnetic shear: Wind observations, *J. Geophys. Res., 102, 19,883-19,895, 1997*.

Reiff, P. H. and J. G. Luhmann, Solar wind control of the polar cap voltage, in '*Solar Wind-Magnetosphere Coupling*', edited Y. Kamide and J.A. Slavin, p. 453, Terra Scientifica, Tokyo, 1986.

Reiff, P.H., T.W. Hill, and J.L. Burch, Solar wind plasma injection at the dayside magnetospheric cusp, *J. Geophys. Res., 82,* 479, 1977.

Richard, R.L., R.J. Walker, and M. Ashour-Abdalla, The population of the magnetosphere by solar wind ions when the interplanetary magnetic field is northward, *Geophys. Res. Lett., 21,* 2455-2458, 1994.

Rijnbeek, R. P., S. W. H. Cowley, D. J. Southwood, and C. T. Russell, A survey of dayside flux transfer events observed by the ISEE 1 and 2 magnetometers, *J. Geophys. Res., 89,* 786-800, 1984.

Rijnbeek, R. P., C. J. Farrugia, D. J. Southwood, M. W. Dunlop, W. A. C. Mier-Jedrejowicz, C. P. Chaloner, D. S. Hall, and M. F. Smith, A magnetic boundary signature within flux transfer events, *Planet. Space Sci., 35,* 871-878, 1987.

Rosenbauer, H., H. Grünwaldt, M.D. Montgomery, G. Paschmann, and N. Skopke, HEOS 2 plasma observations in the distant polar magnetosphere: The plasma mantle, *J. Geophys. Res., 80,* 2723-2737, 1975.

Ruohoniemi J. M., R.A. Greenwald, K.B. Baker, J.-P. Villain, C. Hanuise, and J.D. Kelley, Mapping high latitude plasma convection with coherent HF radars, *J. Geophys. Res., 94*, 13463, 1989.

Russell, C. T., and R. C. Elphic, Initial ISEE magnetometer results: Magnetopause observations, *Space Sci. Rev., 22,* 681-715, 1978.

Russell, C. T., and R. C. Elphic, ISEE observations of flux transfer events at the dayside magnetopause, *Geophys. Res. Lett., 6,* 33-36, 1979.

Sandholt et al., 1996

Sandholt, P.E., C.J. Farrugia, M. Øieroset, P. Stauning, and S.W.H. Cowley, Auroral signature of lobe reconnection, Geophys. Res. Lett., 23, 1725-1728, 1996.

Sandholt, P.E., C.J. Farrugia, J. Moen and B. Lybekk, The dayside aurora and its regulation by the interplanetary magnetic field*, in "Polar Cap Boundary Phenomena ", ed. J. Moen, A. Egeland and M. Lockwood, NATO ASI Series C, Vol. 509*, pp. 189-208 , Kluwer, Dordrecht, 1998.

Sandholt, P.E., C.J. Farrugia, J. Moen, and S.W.H. Cowley, Dayside auroral configurations: responses to southward and northward rotations of the interplanetary magnetic field, *J. Geophys. Res., in press*, 1999

Sanny, J., D.G. Sibeck, C.C. Venturini, and C.T. Russell, A statistical study of transient events in the outer dayside magnetosphere, *J. Geophys. Res., 101*, 4939-4952, 1996.

Saunders, M. A., Recent ISEE observations of the magnetopause and low-latitude boundary layer: A review, *J. Geophys., 52,* 190-198, 1983.

Saunders, M. A., C. T. Russell, and N. Sckopke, A dual-satellite study of spatial properties of FTEs, in *Magnetic Reconnection in Space and Laboratory Plasmas*, *Geophys. Monogr. Ser.*, vol. 30, edited by E.W. Hones Jr., pp. 145-152, AGU, Washington, D. C., 1984a.

Saunders, M. A., C. T. Russell, and N. Sckopke, Flux transfer events, scale size and interior structure, *Geophys. Res. Lett., 11,* 131-134, 1984b.

Savin, S.P., O. Balan, N. Borodkova, E. Budnik, N. Nikolaeva, V. Prokhorenko, T. Pulkkinen, N. Rybjeva, J. Safrankova, I. Sandahl, E. Amata, U. Auster, G. Bellucci, A. Blagau, J. Blecki, J. Buechner, M. Ciobanu, E. Dubinin, Yu. Yermolaev, M. Echim, A. Fedorov, V. Formisano, R. Grard, V. Ivchenko, F. Jiricek, J. Juchniewicz, S. Klimov, V. Korepanov, H. Koskinen, K. Kudela, R.

Lundin, V. Lutsenko, O. Marghitu, Z. Nemecek, B. Nikutowski, M. Nozdrachev¸ S. Orsini, M. Parrot, A. Petrukovich, N. Pissarenko, S. Romanov, J. Rauch, J. Rustenbach, J.A. Sauvaud, E.T. Sarris, A. Skalsky, J. Smilauer, P. Triska, J.G. Trotignon, J. Vojta, G. Zastenker, L. Zelenyi, Yu. Agafonov, V.Grushin, V. Khrapchenkov, L. Prech, O. Santolik, Interball Magnetotail boundary case studies, *Adv. Space Res., 20(4/5),* 999-1015, 1997.

Scholer, M., Magnetic flux transfer at the magnetopause based on single X line bursty reconnection, *Geophys. Res. Lett., 15,* 291-294, 1988a.

Scholer, M., Strong core magnetic fields in magnetopause flux transfer events, *Geophys. Res. Lett., 15,* 748-751, 1988b.

Scholer, M., Asymmetric time-dependent and stationary magnetic reconnection at the dayside magnetopause, *J. Geophys. Res., 94,* 15,099-15,111, 1989.

Scholer, M., P.W. Daly, G. Paschmann, and T.A. Fritz, Field line topology determined by energetic particles during a possible magnetopause reconnection event, *J. Geophys. Res., 87*, 6073, 1982a.

Scholer, M., D. Hovestadt, F.M. Ipavich, and G. Gloeckler, Energetic protons, alpha particles and electrons in magnetic flux transfer events, *J. Geophys. Res., 87,* 2169, 1982b

Sckopke, N., Plasma structure near the low-latitude boundary layer: a rebuttal, *J. Geophys. Res., 96,* 9815-9820, 1991.

Sckopke, N., G. Paschmann, G. Haerendel, B.U.Ö. Sonnerup, S.J. Bame, T.G. Forbes, E.W. Hones Jr., and C.T. Russell, Structure of the low-latitude boundary layer, *J. Geophys. Res. 86,* 2099-2110, 1981.

Semenov, V.S., I.V. Kubyshkin, H.K. Biernat, M.F. Heyn, R.P. Rijnbeek, B.P. Besser, and C.J. Farrugia, Flux transfer events interpreted in terms of a generalized model for Petschek-type reconnection, *Adv. Space Res., 11*(9), 25-28, 1991.

Semenov, V.S., V.V. Lebedeva, H.K. Biernat, M.F. Heyn, R.P. Rijnbeek, and C.J. Farrugia, Time-varying reconnection: Implications for magnetopause reconnection, *J. Geophys. Res., 100,* 21,779-21,789, 1995.

Sharp, R.D., E.G. Shelley, R.G. Johnstone, and A.G. Ghielmetti, Counter-streaming electron beams at ~1R_E over the auroral zone, *J. Geophys. Res., 85,* 92, 1980.

Shue, J.-H., J. K. Chao, H.C. Fu, C.T. Russell, P. Song, K.K.. Kurana, and H.J. Singer, A new functional form to study the solar wind control of the magnetopause size and shape, J. Geophys. Res., 102, 9497, 1997.

Sibeck, D. G., A model for the transient magnetospheric response to sudden solar wind dynamic pressure variations, *J. Geophys. Res., 95,* 3755-3771, 1990.

Sibeck, D.G., Transient events in the outer magnetosphere: Boundary waves or flux transfer events?, *J. Geophys. Res., 97,* 4009-4026, 1992.

Sibeck, D.G., and P.T. Newell, Pressure-pulse driven surface waves at the magnetopause: a rebuttal, , *J. Geophys. Res., 100,* 21,773-21,778, 1995.

Sibeck, D.G. , G. Paschmann, R.A. Treumann, S.A. Fuselier, W. Lennartsson, M. Lockwood, R. Lundin, K.W. Ogilvie, T.G. Onsager, T.-D. Phan, M. Roth, M. Scholer, N. Sckopke, K. Stasiewicz, and M. Yamauchi, Plasma transfer processes at the magnetopause, *Space Science Reviews*, 88, 207-283, 1999

Smith, M.F. and Rodgers, D.J., Ion distributions at the dayside magnetopause, *J. Geophys. Res., 95,* 11617-11624, 1991.

Smith, M.F., and C.J. Owen, Temperature anisotropies in a magnetospheric FTE, Geophys. Res. Lett., 19, 1907-1910, 1992.

Song, P., and C.T. Russell, Model of the formation of the low-latitude boundary layer for strongly northward interplanetary magnetic field, *J. Geophys. Res., 97,* 1411, 1992.

Song, P., R.C. Elphic, C.T. Russell, J.T. Gosling, and C.A. Cattell, Structure and properties of the subsolar magnetopause for northward IMF: ISEE observations, *J. Geophys. Res., 95*, 6375, 1990.

Song, P., G. Le, and C.T. Russell, Observational differences between flux transfer events and surface waves at the magnetopause, *J. Geophys. Res., 99,* 2309-2320, 1994.

Song, P., T.E. Holzer, C.T. Russell and Z, Wang, Modelling the low-latitude boundary layer with reconnection entry, *Geophys. Res. Lett. 21*, 625-628, 1994.

Sonnerup, B.U.Ö., Theory of the low-latitude boundary layer, *J. Geophys. Res., 85*, 2017, 1980.

Sonnerup, B.U.O., G. Paschmann, I. Papamastorakis, N. Sckopke, G. Haerendel, S.J. Bame, J.R. Ashbridge, J.T. Gosling and C.T. Russell, Evidence for magnetic field reconnection at the Earth's magnetopause, *J. Geophys. Res., 86*, 10049-10067, 1981.

Sonnerup, B.U.Ö., I. Papamastorakis, G. Paschmann, and H, Lühr, The magnetopause for large magnetic shear: analysis of convection electric fields from AMPTE/IRM, *J. Geophys. Res., 95,* 10541-10557, 1986.

Southwood, D. J., M. A. Saunders, M. W. Dunlop, W. A. C. Mier-Jedrzejowicz, and R. P. Rijnbeek, A survey of flux transfer events recorded by UKS spacecraft magnetometer, *Planet. Space Sci., 34,* 1349-1359, 1986.

Southwood, D. J., C. J. Farrugia, and M. A. Saunders, What are flux transfer events?, *Planet. Space Sci., 36,* 503-508, 1988.

Spreiter, J.R., A.L. Summers, and A.Y. Alksne, Hydromagnetic flow around the magnetosphere, *Planet. Space Sci., 14*, 223-253, 1966.

Takahashi, K., D.G. Sibeck, P.T. Newell and H.E. Spence, ULF waves in the low-latitude boundary layer and their relationship with magnetospheric pulsations: a multi-satellite observation, *J. Geophys. Res., 96,* 9503-9519, 1991.

Thompsen, M., J. A. Stansberry, S. J. Barne, S. A. Fuselier, and J. T. Gosling, Ion and electron velocity distributions within flux transfer events, *J. Geophys. Res., 92*, 12,127, 1987.

Traver, D.P. D.G. Mitchell, D.J. Williams, L.A. Frank, and C.Y. Huang, Two encounters with the flank low-latitude boundary layer: further evidence for closed field topology and investigation of the internal structure, *J. Geophys. Res., 96,* 21,025-21,035, 1991.

Treumann, R.A., J. La Belle, and R. Pottelette, Plasma diffusion at the magnetopause: the case of lower hybrid drift waves, *J. Geophys. Res., 96,* 16,009-16,013, 1991.

Treumann, R.A., J. LaBelle, and T.M. Bauer, Diffusion processes: an observational perspective, in *Physics of the magnetopause*, Geophys. Mono. 90, ed. P. Song, B.U.Ö. Sonnerup and M. Thompsen, pp. 331-341, 1995.

Vasyliunas, V.M., Interaction between the magnetospheric boundary layers and the ionosphere, in *Proceedings of the Magnetospheric Boundary Layers Conference, Alpbach*, *Eur. Space Agency Spec Publ.*, *ESA SP-148*, 387-394, 1979.

Williams, D.J., D.G. Mitchell, T.E. Eastman and L.A. Frank, Energetic particle observations in the low-latitude boundary layer, *J. Geophys. Res., 90*, 5097, 1978.

Wild J.A. et al., *Annales Geophys.*, This issue, 2001

Wing, S., P.T. Newell, and T.G. Onsager, Modelling the entry of the magnetosheath electrons into the dayside ionosphere, J. Geophys. Res., 101, 13155-13168, 1996.

Winske, D., V.A. Thomas, and N. Omidi, Diffusion at the magnetopause: A theoretical perspective, in *Physics of the Magnetopause*, *Geophys. Monogr Ser.,* vol. 90, edited P. Song, B.U.Ö. Sonnerup, and M. F. Thomsen, pp. 321-330, AGU, Washington, D.C., 1995.

Woch, J., and R. Lundin, The low-latitude boundary layer at mid-altitudes: Identification based on Viking hot plasma data, *Geophys. Res. Lett., 20*, 979-982, 1993.

Woch, J., M. Yamauchi, R. Lundin, T.A. Potemra and L.J. Zanetti, The low-latitude boundary layer at mid altitudes: relation to large-scale Birkeland currents, *Geophys. Res. Lett.* **20**, 2251-2254, 1993.

Woch, J., R. Lundin, T.E. Potemra and M. Shapshak, The projection of the magnetospheric boundary layers to mid-altitudes, J.A. Holtet and A. Egeland (eds), *Physical Signatures of Magnetospheric Boundary Layer Processes*, 83-97, Kluwer, 1994.

Xu, D., M.G. Kivelson, R.J. Walker, P.T. Newell and C.-I. Meng, Interplanetary magnetic field control of mantle precipitation and associated field-aligned currents, *J. Geophys. Res.*, *100*, 1837-1846, 1995.

Legends to figures

Figure 1. Observation of transient events seen by Cluster and the EISCAT Svalbard Radar (ESR) on 14 January 2001. (a). The plasma concentrations seen in the ionosphere along the low elevation (30°), poleward beam of the ESR, colour coded as a function of time and latitude. The centre of poleward-moving events are marked with a black line which are numbered in continuation of the events earlier ion the same day, as studied by *Lockwood et al.* (2001, this issue). (b). The observations along the field-aligned ESR beam, shown as a function of time and altitude. (c) An energy-time spectrogram of differential energy flux of ions, integrated over all pitch angles, as observed by the CIS instrument on Cluster C3. (d) An energy-time spectrogram of the count rate of electrons observed by the HEEA detector of the PEACE instrument on Cluster C3 in zone 11 (electrons moving in the $+Z_{GSE}$ direction). The ESR and CIS data are colour coded using the same scales as in figure 1 of *Opgenoorth et al.* (2001, this issue). The PEACE data are scaled on the same scale as used in Figure 8 of the present paper. The vertical dashed lines give the times of closest conjunction of the ESR and Cluster (mauve) and the ESR and the DMSP-F15 satellite (green).

Figure 2. The magnetic field observed by the four Cluster Craft at 11-16 UT on 14 January 2001. The plots shows the B_X, B_Y and B_z components in the GSE frame and the field magnitude |B|. Data from craft C1, C2, C3 and C4 are coloured (respectively) black, red, green and magenta. (N.B. in this figure, data have been plotted in the order C1, C2, C3 and then C4 and, because the data are very similar on this time scale, the magenta line for C4 has covered much of the other three lines).

Figure 3. (a) the PEACE data shown in figure 1(d) and compared with (b) the IMF clock angle θ_{IMF} in GSM coordinates, as observed by ACE and (c) the solar wind

dynamic pressure, P_{SW}, also observed by ACE. The ACE data are plotted against lagged time, using the nominal 75 min. lag derived independently by *Lockwood et al.* (2001, this issue) and *Opgenoorth et al.* (2001, this issue) for, respectively, before and after the period of interest in this paper. An additional lag of 16.5 min has been introduced to get a good correspondence between the transient LLBL entries seen by Cluster and the increases in θ_{IMF} to near 90°.

Figure 4. Energy-time spectrograms for (a) electrons and (b) ions observed by DMSP-F15 as it passed equatorward in close conjunction with the ESR along the path shown in figure 5. In both cases, the differential energy flux is plotted as a function of energy (increasing upward) and observation time, t_s. (c) shows the vertical (green) and horizontal (purple) components of the ion velocity (the horizontal component being perpendicular to the satellite track such that positive values have a sunward component and negative values an antisunward component. The orange-and-black dashed line gives the time of closest conjunction with the ESR field-aligned beam and the red-and-black line gives the open-closed field line boundary (OCB) defined from the energetic magnetospheric electrons.

Figure 5. An invariant-latitude (Λ) – MLT map of the convection equipotentials from the AMIE technique for magnetometer, SuperDARN, EISCAT/ESR and DMSP data post-integrated over the interval 11:40-11:45. The path of the DMSP-F15 satellite is shown, the two thick segments showing where the satellite observed sunward convection and inverted-V electron precipitation and magnetosheath electron precipitation shown. The location of the open-closed boundary (OCB, crossed by DMSP-F15 at 11:45) is also marked as, are the locations of the two ESR beams and the mapped footprint of the Cluster spacecraft.

Figure 6. The sequence of 5-minute integrated AMIE convection patterns for 11:05-11:45. The locations of the two ESR beams are shown in each panel.

Figure 7. (a)-(c), the lagged (by 75 min) variations of the IMF components B_X, B_Y and B_Z in the GSM reference frame;(d) the energy-time spectrogram of the electron data seen by PEACE-C4 (as shown in figures 1 and 3), and (e) the "upward continuation" of the X component of the magnetic field B_X' as a function of latitude and from the IMAGE magnetometer chain. The technique used to derive B_X' employs Fourier analysis of the observations of the data from the latitudinal chain of stations on the ground to reconstruct high-resolution latitude variations that would have been observed just below the current layer.

Figure 8. Observations of the electrons and ions made by the PEACE and CIS instruments of the Cluster craft at 11:19-11:27. (a)-(d) are energy-time spectrograms of count rates seen by the HEEA detector of PEACE in zone 11 (electrons moving in the $+Z_{GSE}$ direction) for spacecraft C1, C2, C3 and C4, respectively. (e)-(g) energy-time spectrograms of differential number flux observed by CIS for spacecraft C1, C3 and C4. The arrows mark the boundaries of the LLBL event, defined from the lowest energy sheath electrons, and plotted for the same times on the ion spectrograms and in figure 10.

Figure 9. The moments of the ion gas from spacecraft C3 for the interval shown in figure 8. The panels show: (a) the proton number density, $N(H^+)$; (b) the alpha particle number density, $N(He^{++})$; (c) the field-parallel ion temperature, $T_{||}$; (d) the field-perpendicular ion temperature, $T_\perp$; and the ion velocity components (e) V_X, (f) V_Y, and (g) V_Z, in GSE coordinates.

Figure 10. The spacecraft potentials in the interval shown in figure 8, measured by the EFW instruments on spacecraft C1 (black), C2 (red), C3 (green) and C4 (blue). The arrows correspond to those plotted in figure 8.
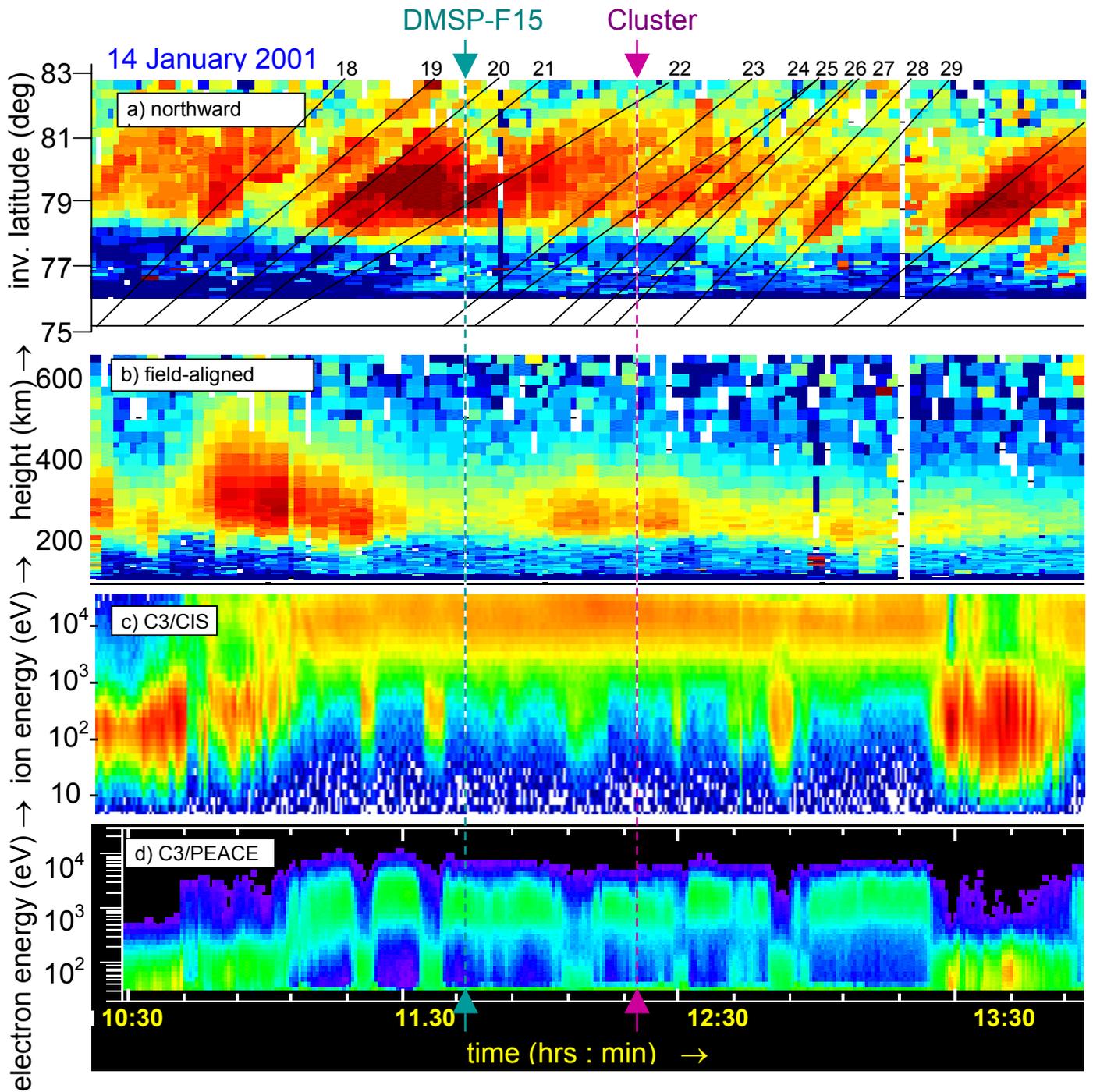

Figure 11. The magnetic field observed by the four Cluster Craft during 11:19-11:27 UT on 14 January 2001. The plots shows the B_L, B_M and B_N components (in the boundary-normal frame described in the text) and the field magnitude |B|. Data from craft C1, C2, C3 and C4 are coloured (respectively) black, red, green and magenta.

Figure 12. Same as Figure 8 for the interval 12:00 - 12:20 UT.

Figure 13. One-minute integrations (shown every 2 minutes) of 630 nm emissions seen by the Norwegian all-sky camera at Ny Ålesund, Svalbard. Each frame shows the outline of Svalbard and the east coast of Greenland and lines of constant geographic latitude and longitude and the mapped footprint of the Cluster craft. Al emissions have been mapped assuming an emission altitude of 250 km. The images are ordered from left to right in each row and rows are ordered from top to bottom. The first image (top left) is for 12:00 and the last (bottom right) for 12:34 UT.
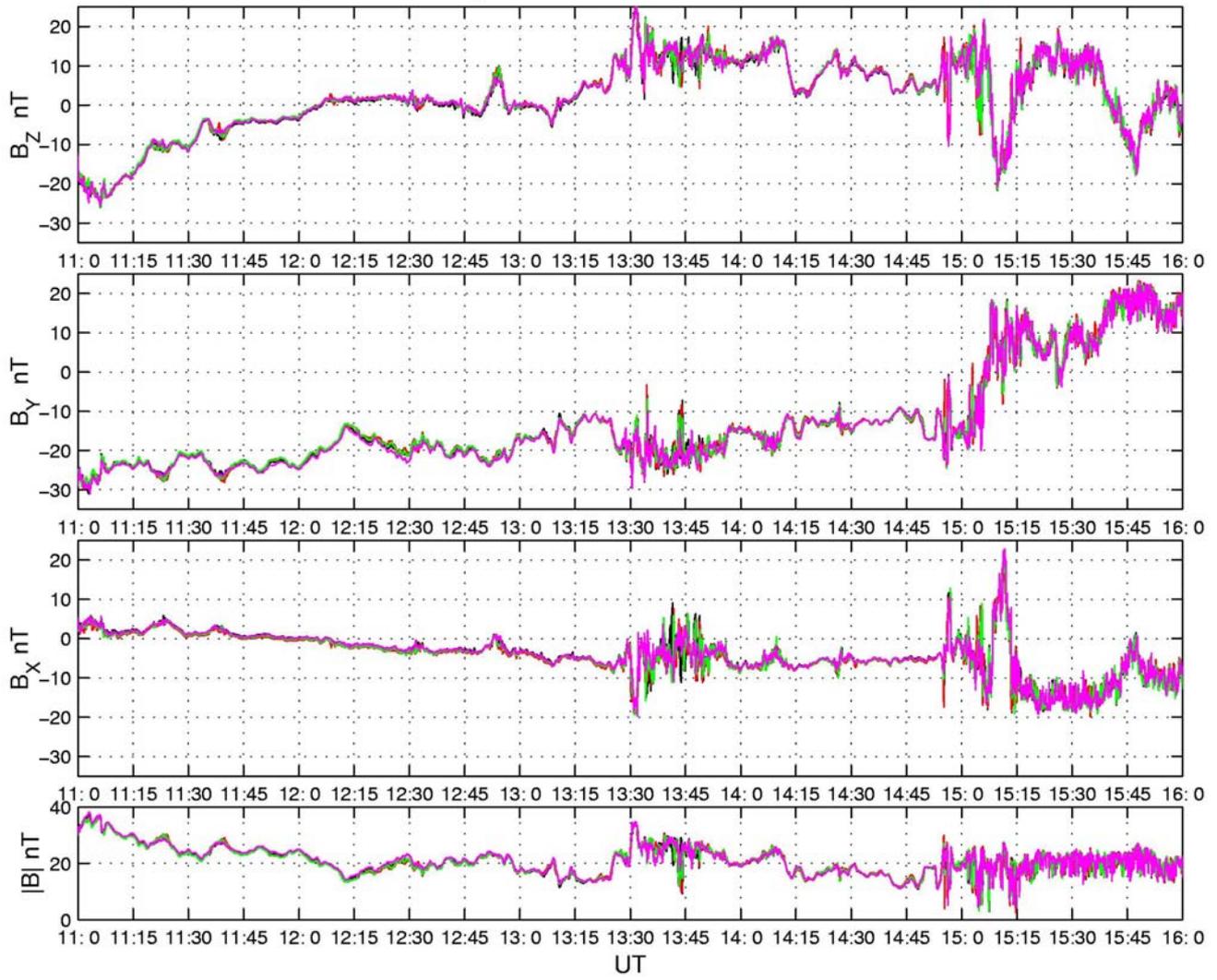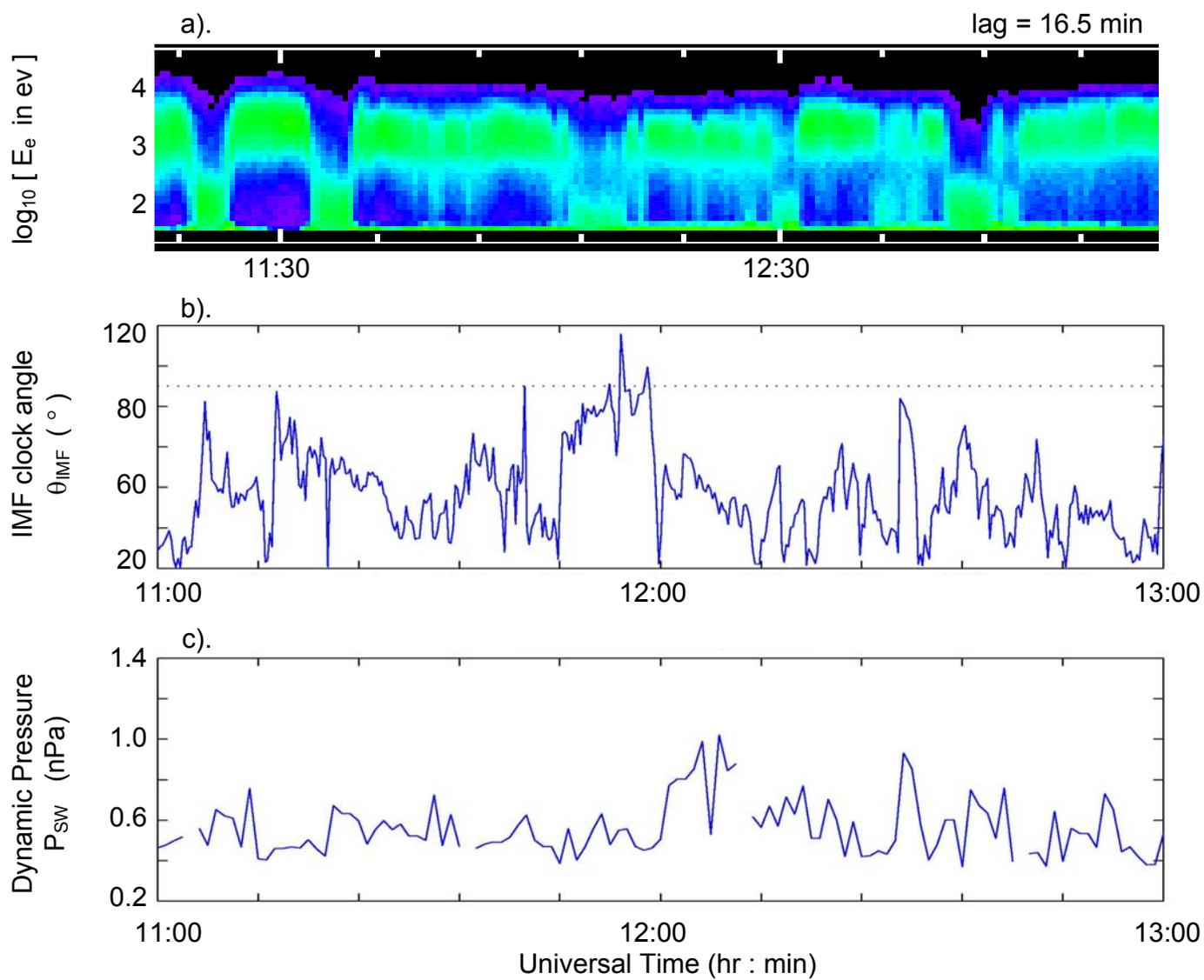
Figure 14. The same as figure 11, for the interval 12:45-13:00 UT.
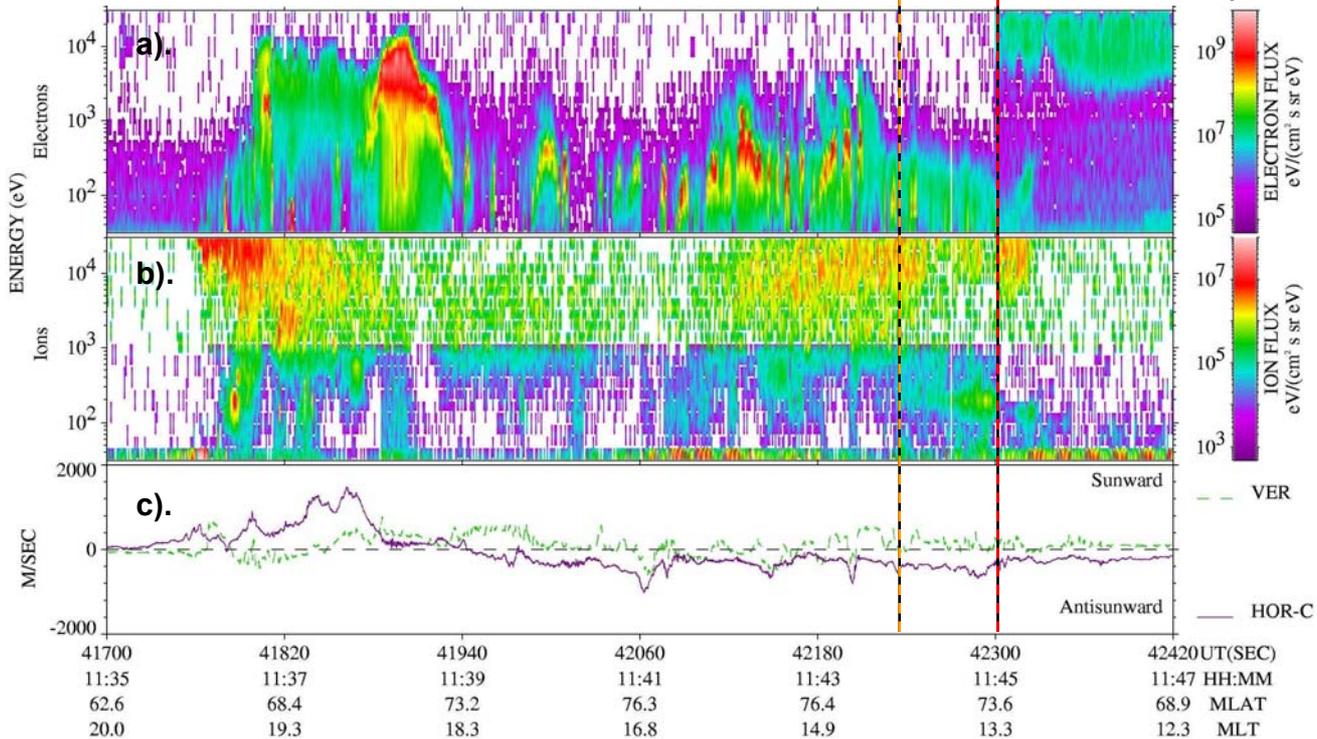
14 January 2001

Cluster　　　Magnetic field　GSE　　　2001 Jan 14

a).   lag = 16.5 min

b).

c).

DMSP-F15

ESR field-aligned beam

Cluster footprint

ESR low elevation beam

12

OCB

Λ = 60°

70°

sheath-like electrons

+10kV

+20kV

18

06

-5kV

0 kV

35kV
11:40 UT
14 January 2001

inverted-V electrons

MLT = 00 hrs

2001 JAN 14 11:05 UT   12   ELECTRIC POTENTIAL 55 kV
MH I 6
HPI = 6   50°
18   06
00

2001 JAN 14 11:10 UT   12   ELECTRIC POTENTIAL 49 kV
MH I 7
HPI = 7   50°
18   06
00

2001 JAN 14 11:15 UT   12   ELECTRIC POTENTIAL 39 kV
MH I 7
HPI = 7   50°
18   06
00

2001 JAN 14 11:20 UT   12   ELECTRIC POTENTIAL 47 kV
MH I 7
HPI = 7   50°
18   06
00

2001 JAN 14 11:25 UT   12   ELECTRIC POTENTIAL 34 kV
MH I 7
HPI = 7   50°
18   06
00

2001 JAN 14 11:30 UT   12   ELECTRIC POTENTIAL 34 kV
MH I 7
HPI = 7   50°
18   06
00

2001 JAN 14 11:35 UT   12   ELECTRIC
                              POTENTIAL
                              35 kV
MH I 7
HPI = 7   50°

18   06

                        00

2001 JAN 14 11:40 UT   12   ELECTRIC
                              POTENTIAL
                              35 kV
MH I 7
HPI = 7   50°

18   06

                        00

2001 JAN 14 11:45 UT   12   ELECTRIC
                              POTENTIAL
                              36 kV
MH I 6
HPI = 6   50°

18   06

                        00

a). B_X (nT)

b). B_Y (nT)

c). B_Z (nT)
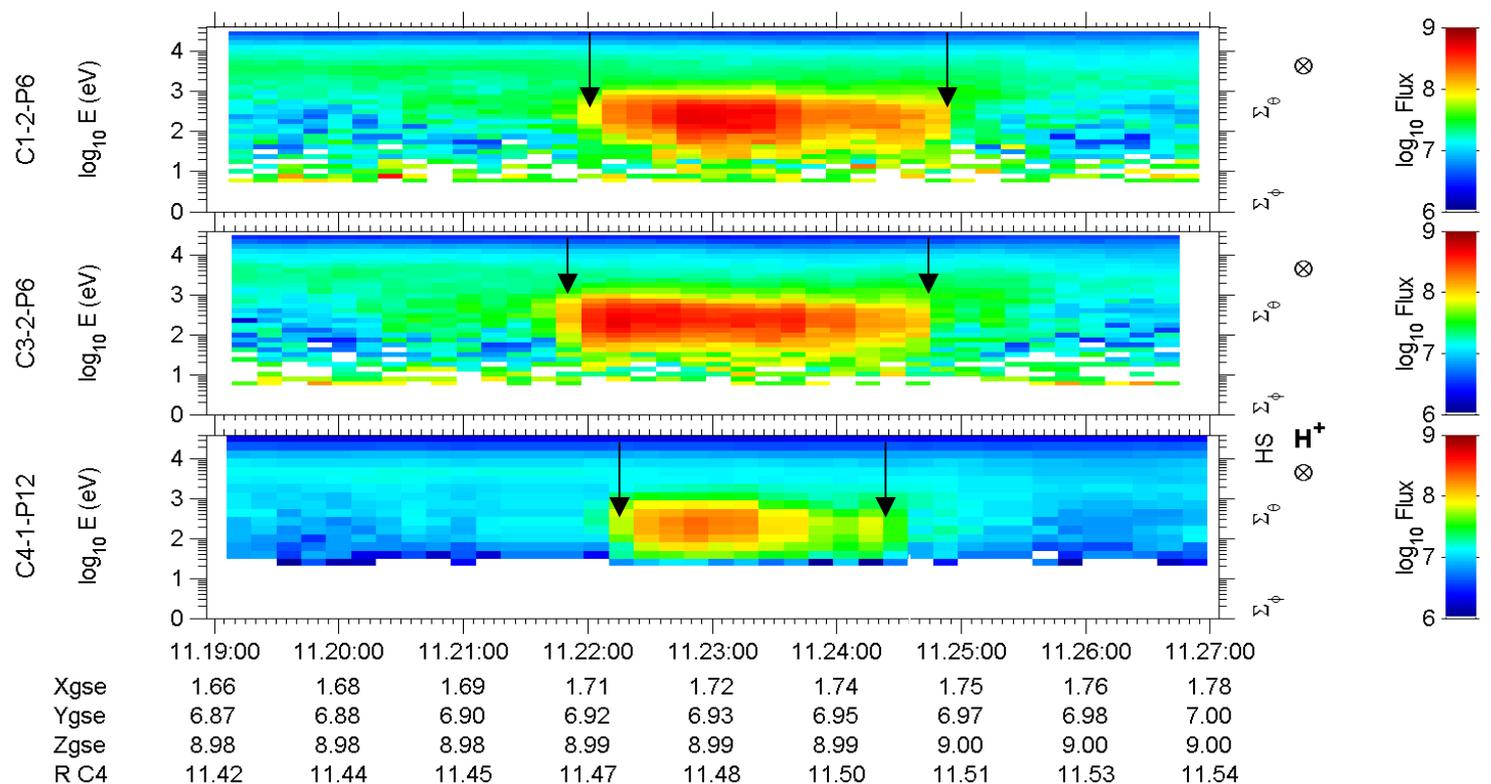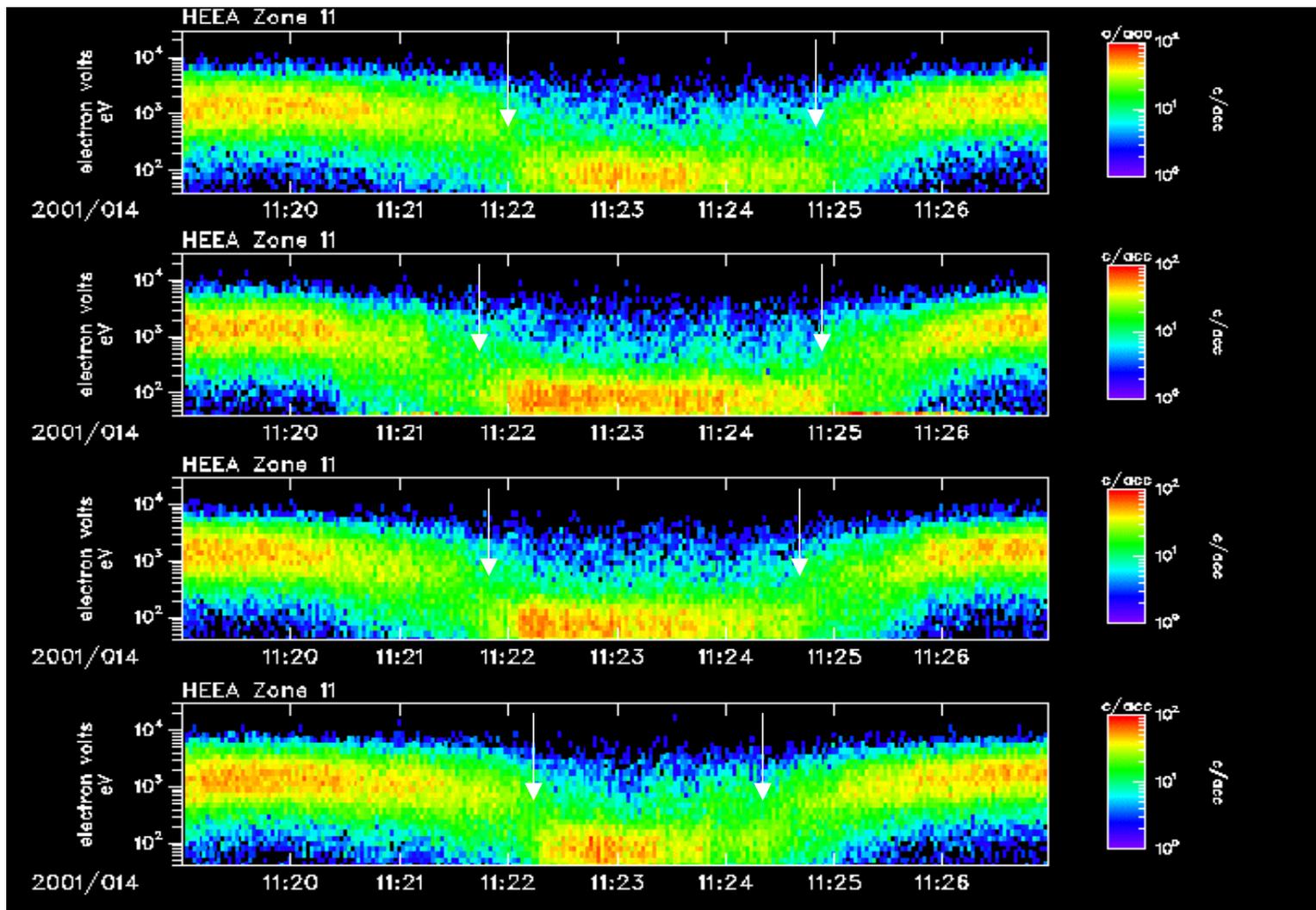
d).

e).

Geomagnetic Latitude →

$B_{X'}$ (nT)

Universal Time (hrs: min)

14 January 2001, Cluster C4–CIS

Cluster   FGM (minimum variance)   2001 Jan 14

Cluster   FGM (minimum variance)   2001 Jan 14